Accepted manuscript of Microchem. J. 107 (2013) 47-62

http://doi: 10.1016/j.microc.2012.07.002

Application of the electronic spectra of porphyrins for analytical purposes: the effects of metal ions and structural distortions

Zsolt Valicsek* and Ottó Horváth

Department of General and Inorganic Chemistry, Institute of Chemistry, Faculty of Engineering, University of Pannonia, P.O.B. 158, Veszprém H-8201, Hungary

Abstract

We investigated the UV-Vis absorption, singlet-1 and singlet-2 fluorescence, as well as the formation of several metalloporphyrins from equilibrial and kinetic aspects in aqueous solution. Among these complexes were numerous typical out-of-plane and several in-plane metalloporphyrins, and between the two categories, a few border-line cases. On the basis of our results, we have complemented the categorization introduced by Barnes and Dorough for the metalloporphyrins. According to our observations, also in metalloporphyrins, the distortion, i.e., the planarity or nonplanarity of the macrocycle, is basically responsible for the spectral characteristics, while the electronic structure of metal center is a secondary factor, with a considerable importance mainly in the in-plane complexes. The type of complexes can be spectrophotometrically determined on the basis of their UV-Vis absorption and fluorescence spectra. Beside the spectral and photophysical effects of metalation, also those of the structural distortions were studied, which can originate also from metalation, protonation or overcrowded peripheral substitution of the free-base porphyrins, as well as from the axial ligation of metalloporphyrins.

Our observation may be useful for different spectrophotometric analytical detection and determination methods, e.g. size-selective metal detection using free-base porphyrins (or other ringed chelate ligands), as well as the determination of Lewis bases as potential axial ligands, using metalloporphyrins.

Keywords: spectrophotometric detection, metalloporphyrins, distortion, UV-Vis absorption, S_1- and S_2-fluorescence, LoD and ToD.

* Corresponding author. Tel.: +36 (88) 624 431; fax: +36 (88) 624 548 (Z. Valicsek).
E-mail addresses: valicsek@vegic.uni-pannon.hu (Z. Valicsek), otto@vegic.uni-pannon.hu (O. Horváth).

1. Introduction

Porphyrins and their derivatives represent one of the most significant families of compounds in biochemistry. Four pyrroles are connected to each other through methylidine bridges, forming the porphin ring (Fig. 1). It has a planar structure with extended conjugated π-electron system and aromatic character, as well as a size-limited coordination cavity for binding of different metal ions. They are the strongest light-absorbing materials in Nature, therefore they are also called as "the pigments of the life" [1].

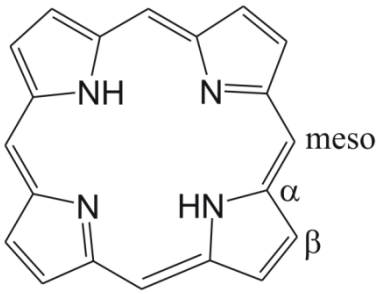

Fig. 1. The porphin ring with the symbols of carbon atoms. The numeration of the carbons starts from an α-atom to a β-carbon, hence, every fifth numbers belong to meso-carbons.

The substituted porphins are called porphyrins. Natural porphyrins are substituted usually on (β) pyrrole-carbons connecting to proteins, however, the simplest synthetic derivatives contain substituents in the meso-positions.

1.1. Porphyrins in Nature

Free-base or metal-free porphyrins exist in Nature too: pheophytin, coproporphyrin, uroporphyrin (I and III isomers), protoporphyrin-IX (and open-chain tetrapyrroles are the bile pigments, e.g. bilirubin, biliverdin) [2].

However, the metalloporphyrins play more essential roles, mainly magnesium(II) chlorins in chlorophylls and bacteriochlorophylls, iron(II) protoporphyrin in hemoglobin, iron(III) protoporphyrins in myoglobin, cytochromes, oxidase, peroxidase, catalase, and oxoanion reductase enzymes. Moreover, hemovanadin (V), pinnaglobin (Mn), and coboglobin (Co) can function as O_2 carriers in inferior organisms. The F430 cofactor of methyl reductase is the most reduced ringed tetrapyrrole in Nature {nickel(II)-dodecahidroporphyrin} [3, 4] (Fig. 2).

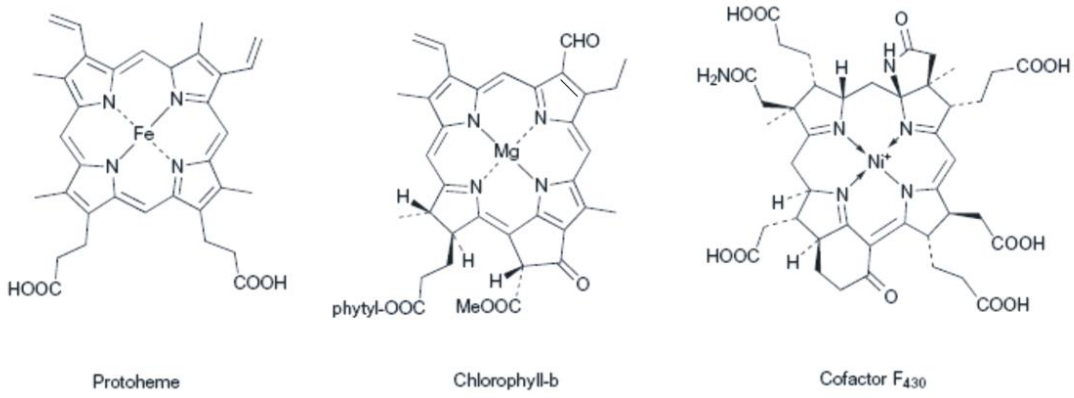

Fig. 2. Most important metalloporphyrins in Nature [3].

Cobalamin in vitamin B_{12} is a cobalt(II)-corrole (in the corrin ring there is a direct bond between two pyrroles instead one of the methylidine bridges). The strong chelating effect of ringed tetrapyrroles can cause the hyperaccumulation of rare metal ions in living cells [5], and also in the lifeless environment: nickel and vanadium (rarely manganese and gallium) porphyrins as decomposition products of chlorophylls and hems can occur in kerogens, crude oils, coals, oil shales, bitumens, asphaltenes. Therefore these molecules are the main evidences for the biogenic origin of these materials [6, 7]. Chlorins (and benzoporphyrins) were spectroscopically detected in the interstellar space too [8].

1.2. Distortion of porphyrins

In porphyrins the conjugation would favour planar structure, however, geometrical distortion can arise owing to the peripheral substituents or the metal center (originating from its size or its axial ligand). It certainly has effects on the enzyme functions: in the hemoglobin the iron(II) metal center without oxygen is in a high spin, quintet state and located out of the plane of the four pyrrolic nitrogens because of the axial coordination of a hystidine. This coordination results in the dome distortion of the macrocycle. Due to the O_2 binding to the metal center from the opposite side of the porphyrin, Fe^{2+} turns into its low spin, singlet state and sinks into the plane. The deformation of the macrocycle ceases, therefore the quaterner structure of the protein changes, as well as further oxygen bindings of the three other heme-units (two α– and two β-chains in a hemoglobin) are accelerated in 1:4:24:9 successive binding proportion. The deformation of bacteriochlorophyll promotes the faster electron transfer [3].

Moreover, in the biosynthesis of metalloporphyrins, the aminoacids of the metal ion inserting enzymes (ferro-, magnesium-, nickel-, cobalt-chelatase, siroheme-synthase) distort the porphyrins to a saddle shape to enhance the incorporation of metal ion because generally this is the rate determining step in the metalation of the protonated, ringed and tetradentate ligand [9].

In chemical researches, the distortion of porphyrins can modifiy their redox potentials, basicity, reactivity, catalytic activity, coordinative abilities toward metal ions, as well as, in the case of metalloporphyrins, the affinity of metal center towards axial ligands. Also as a consequence of distortion, the symmetry decreases, resulting in typical spectral changes in several ranges of the electromagnetic spectrum [3].

The most characteristic types of distortions are saddle, dome, ruffled and wave (chair-like) (Fig. 3), while the less frequent ones are propeller and helical, however, their combinations may also occur (e.g. sadruf, gabled or puckered) [3].

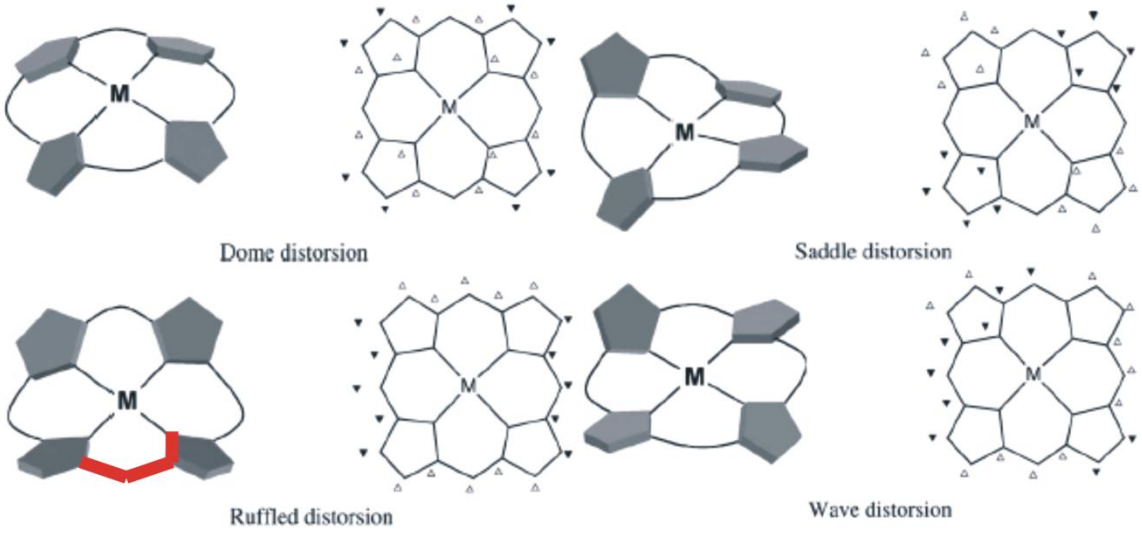

Fig. 3. The most typical distortions [14]. The widely used dihedral angle as a measure of distortion is represented on the image of the ruffled type [3].

The overcrowded (octa- or dodeca-) substitution on the periphery [10, 11], the protonation or alkylation of the pyrrolic nitrogens [12], or the too short metal-nitrogen bonds (significantly shorter than 2 angströms) through the contraction of the coordination cavity can result in the ruffled or saddle deformation. The typical examples for the latter ones are the low-spin nickel(II) [4, 13], chromium(III) [14, 15], titanium(IV) [16] and manganese(III) porphyrins [17], as well as the copper(III) corrole [18], while their high-spin complexes (if it is possible) are usually planar.

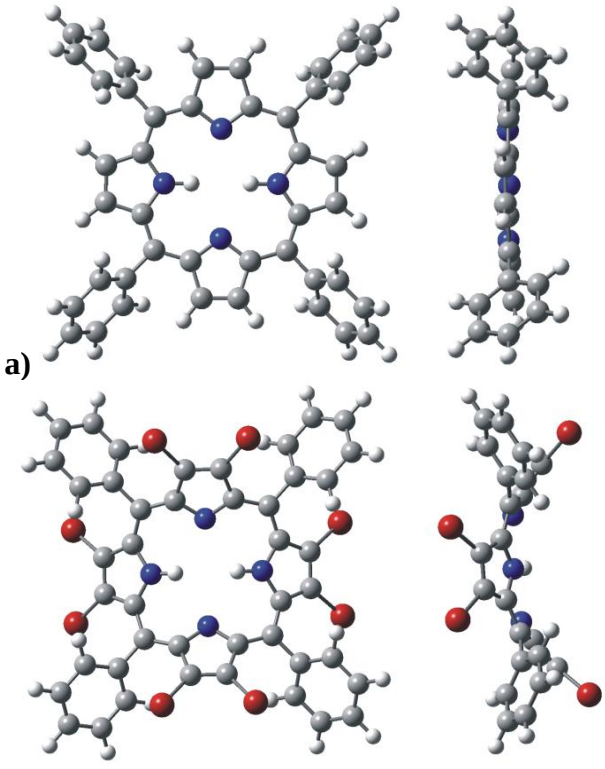

Fig. 4. The structure of 5,10,15,20-tetraphenyl-porphyrin, H_2TPP (a); and that of its 2,3,7,8,12,13,17,18-octabrominated derivative, H_2TPPBr_8 (b) [10].

Conversely, if the M-N bonds are considerably longer than one-half of the diagonal N-N distance in the free-base porphyrin, dome deformation can take place. This occurs if the radius of the metal center exceeds the critical value of about 75-90 pm (depending on the type of porphyrin ligand), or it does not prefer the square planar coordination. Such metal ions do not fit into the cavity of the ligand, and are located above the plane of the pyrrolic nitrogens [19, 20]. Furthermore, a smaller metal ion can also possess an out-of-plane position, therefore causing a dome distortion if it coordinates axial ligand(s) from only one side of the porphyrin plane (similarly to the hemoglobin without O_2 coordination) [21].
Ruffled and saddle distortions result in a stronger deviation from the plane than dome distortion does, which is confirmed by the widely used measure of distortions, the N–C_α–C_{meso}–C_α' dihedral angles too [3] (demonstrated in Fig. 3). Consequently, for the dome distortion we had to define a more suitable, informative parameter, the domedness: the distance between the plane of the pyrrolic nitrogens and that of the β-carbons [22].

Porphyrins and their derivatives are the strongest light-absorbing materials not only in Nature, therefore the ultraviolet-visible spectrophotometry is one of the most fundamental, yet most informative spectroscopic methods in the porphyrin chemistry because it gives information about the electronic structure as well as the chemical features of the molecules even at very low concentrations [23]. Owing to the rigidity of the porphyrins' ringed structure, beside the electronic factors, also steric effects have influences on the spectra. "The most commonly observed spectroscopic consequence of porphyrin nonplanarity is a redshift in the ππ* absorption bands in the UV–visible spectrum… The size of the redshift is proportional to the magnitude of the distortion, albeit in a nonlinear fashion..." [3]. In arylated porphyrins, the distortion can result in the extension of delocalization by the twisting of aryl substituents from almost perpendicular orientation closer to the porphyrin plane (Fig. 4).
The redshifts of absorption bands induce those of the emission bands too, and as further consequences of distortion, the quantum yields and the lifetimes of the fluorescences decrease due to the acceleration of non-radiative decays [24].
Considering the consequences of distortions as steric effects in the metalation of porphyrins, we disproved the validity of the widespread categorization method of metalloporphyrins introduced by Gouterman and based exclusively on the electronic structure of metal center [25]. Instead, we declared the distorting effect originating from the size and the position of the metal center compared to the cavity of the ligand as the primary aspect [19]. It was already suggested by Barnes and Dorough [26] on the basis of the behaviour of metal ions in the metal exchange reactions: the inert in-plane complexes (where the metal center is located in the plane of porphyrin), the labile out-of-plane complexes (Fig. 5), and the border-line cases, e.g., zinc(II) and magnesium(II) porphyrins, in which the metal center is in the plane but with ionic character in bonding, therefore it can be easily exchanged. This categorization of metalloporphyrins based on the metal exchange reactions was confirmed by the investigation of the acid solvolysis reactions: the reaction rate constants proved to be correlated with the lability of complexes: Cd^{2+}>Mg^{2+}>Mn^{2+}>Fe^{2+}>Zn^{2+} >> Co^{2+}>Cu^{2+}>Ni^{2+} [27]. We complemented this categorization aspect with the experiences from distortion that also in metalloporphyrins the planarity or nonplanarity of the macrocycle is basically responsible for spectral characteristics; the electronic structure of metal ions is secondary, mainly in the in-plane complexes.

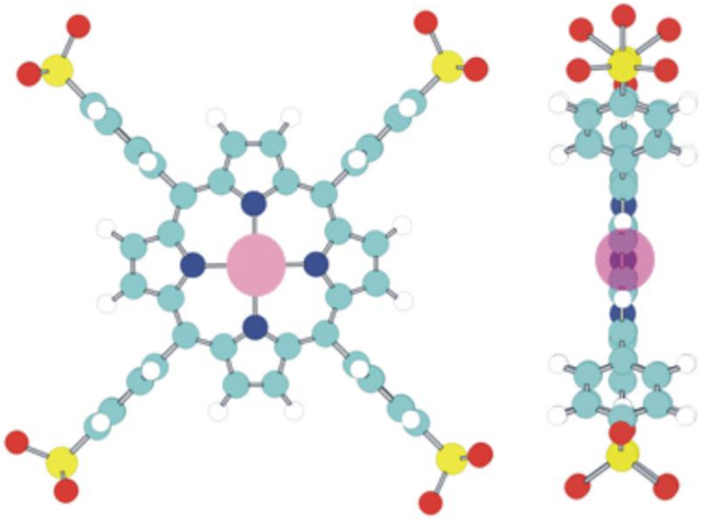

a)

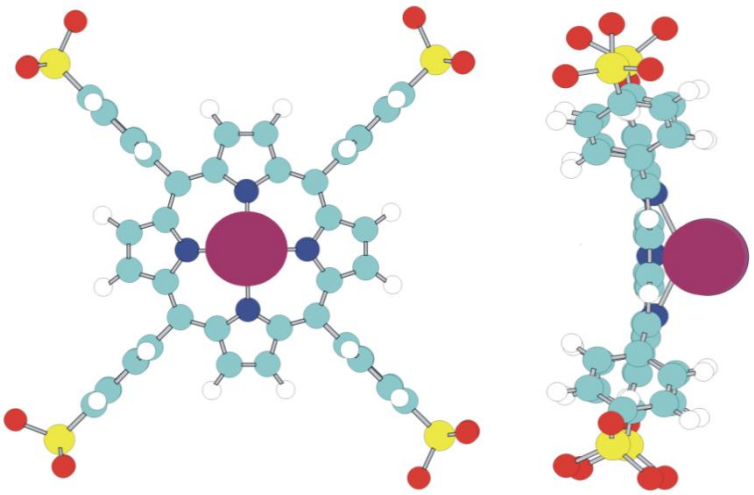

b)

Fig. 5. Structure of an in-plane metallo-TSPP {TSPP=5,10,15,20-tetrakis(4-sulphonatophenyl)porphyrin} (a);
and that of an out-of-plane metallo-TSPP (b) [19].

1.3. Analytical applications of porphyrins

The structural as well as the spectroscopic and electronic effects of the metalation for the free-base porphyrins make the highly sensitive detection of metal ions (10^{-7} – 10^{-5} M) possible, mainly in spectrophotometric, electrochemical or chromatographic methods [28] (however, a lot of interferences between the ions in the systems studied can occur). "The large molar absorption coefficient and very high stability of the metalloporphyrins are very useful for the highly sensitive analysis of trace amounts of metal ions, and the size selectivity of the porphyrins is valuable for the separation of various kinds of metal ions" [29]. Some methods are based on the simple measurement of UV-Vis absorption of porphyrins (which belong to the strongest light-absorbing chelate ligands [30]), e.g. for mercury(II) [31], other post-transition metal ions (Cd^{2+}, Zn^{2+}, Pb^{2+}, Cu^{2+}) [32], manganese(II) and (III) [33], cobalt(II) (using photolabile cadmium(II) porphyrin) [34]. For detection of platinoid metal ions in trace amounts, an indirect spectrophotometric process was developed by the degradation of water-soluble porphyrins in the reaction with oxidants, catalysed by noble metal ions [35, 36].

Several fluorometric procedures are widely used, e.g. for Ca^{2+} [37], Hg^{2+} [38], Cd^{2+} and Pb^{2+} ions in 10^{-7} M concentration [39], and for Hg^{2+} and Fe^{2+} by fluorescence resonance energy transfer [40]. In HPLC techniques heavy metal ions can be determined by porphyrins [28], as well as nickel and vanadium ions from the crude oils too [7]. In the determination of larger heavy metal ions (e.g. Pb^{2+}), which can form only labile out-of-plane metalloporphyrins, also the interference of smaller ones (e.g. Cu^{2+}), which form kinetically inert in-plane complexes, can be suppressed by adding of the suitable porphyrins [41].

Using free-base porphyrins, the measurement of pH [42] as well as the humidity [43] can be solved, while for the detection of other molecules, mainly Lewis bases as potential axial ligands, metalloporphyrins can be more effective than free-base porphyrins. Anion-selective polymer membrane was produced by use of the porphyrin complexes of the third main group metal ions [44], as well as anion-sensing nanoparticles by zinc(II) porphyrins [45]. However, free-base porphyrins can also be applied for the selective determination of anions, such as fluoride [46], bromide [47] and nitrite [48].

Moreover, porphyrins in films and membrans are widely used for sensing of gases: e.g. oxygen [28, 49, 50], nitrogen oxides [28, 51, 52, 53], carbon monoxide [52], carbon dioxide [54], hydrogen chloride [55], and ammonia [56]. The simultaneous determination of oxygen and

carbon dioxide [54], oxygen and temperature [49] as well as oxygen and hydrogen peroxide [50] can be implemented too.
Numerous analytical methods for determination of organic compounds were developed by utilization of porphyrins: e.g. for nucleic acids [28, 42, 57, 58, 59] (porphyrin exciton coupled circular dichroism [57] for other chiral agents too), aminoacids and proteins [48, 60, 61], carbohydrates [28, 62, 63], phenols and chlorophenols [64], phenolic endocrine compounds [65], hormones [66], non-ionic surfactants [67], phospholipids [68], sulphur-containing hydrocarbons [48, 69], and explosives [70].
Most of these analytical methods are based on the spectrophotometric properties (absorption, light scattering and fluorescence) of porphyrins, therefore in this work we would like to summarize and complement the knowledge in this area of porphyrin-chemistry from analytical aspects. In this paper the effects of metalation, axial coordination and distortion are demonstrated and explained. We investigate water-soluble porphyrins because the complexes with very different metal ions can be more simply produced in aqueous systems than in organic solvents [10, 19, 20, 22, 71-79]. In these respects one of the best free-base ligands is the anionic 5,10,15,20-tetrakis(4-sulphonatophenyl)porphyrin (H_2TSPP^{4-}, Fig. 5) because its negative charge enhances the coordination of positively charged metal ions. Furthermore, this ligand is the most widely used analytical reagent among the porphyrin derivatives [28, 35, 36, 42, 59, 60, 65]. However, our spectrophotometric conclusions can be adapted for other porphyrins too.

2. Experimental

Analytical grade tetrasodium 5,10,15,20-tetrakis(4-sulfonatophenyl)porphyrin ($C_{44}H_{26}N_4O_{12}S_4Na_4 \cdot 12H_2O$ = $Na_4H_2TSPP \cdot 12H_2O$) (Sigma–Aldrich) and simple metal salts such as perchlorate, chloride, nitrate or sulphate were used for the experiments. The solvent was double-distilled water purified with Millipore Milli-Q system. The pH of most of the metalloporphyrin solutions was adjusted to 8 by application of borate buffer, also keeping the ionic strength at the constant value of 0.01 M. Exceptions were iron(II) [75], silver(I) [77], bismuth(III) [78], and lanthanide(III) ions, in the solutions of which the pH was regulated to 6, and the ionic strength to 1 M by acetate buffer to hinder the hydrolyses (and in the case of Fe^{2+} to hinder its exchange reaction with Fe^{3+}). Also pH≈6 and I=1 M was adjusted by sodium chloride in the solutions of thallium(III) [74]. In the investigation of metalation of H_2TSPP^{4-}, pH lower than 6 could not be applied because the protonation of the ligand, H_4TSPP^{2-} (pK_3 = 4.99, pK_4 = 4.76 [80]) hinders the complex formation.
Octabrominated free-base porphyrin, $H_2TSPPBr_8^{4-}$ was utilized to investigate the effect of saddle distortion of the macrocycle (Fig. 4, the ionic sulphonate groups have insignificant effect on the structure and the spectral data) [10].
We determined the spectral data (molar absorption, fluorescence quantum yields and lifetimes) of metalloporphyrins by using the free-base ligands as references.
The absorption spectra were recorded and the photometric titrations were monitored by using a Specord S-100 and a Specord S-600 diode array spectrophotometer. For the measurement of fluorescence spectra a Perkin ELMER LS 50-B and a Horiba JobinYvon Fluoromax-4 spectrofluorometer were applied. The latter equipment supplemented with a time-correlated single-photon counting (TCSPC) accessory was utilized for determination of fluorescence lifetimes, too. Rhodamine-B and $Ru(bpy)_3Cl_2$ were used as references for correction of the detector sensitivity and for determination of the fluorescence quantum yields of H_2TSPP^{4-} [74]. Luminescence spectra were corrected for detector sensitivity. For the elimination of the potential reabsorption effects in the detection of luminescence, low concentration or a holder for solid samples were applied. Because of the small Stokes-shifts and the disturbing effect of the (Rayleigh and) Raman scattering, the spectrum analyses were carefully carried out by fitting Gaussian and Lorentzian curves in MS Excel.

3. Results and discussion

Porphyrins have two $\pi\pi^*$ electronic transitions in the visible region of the electromagnetic spectrum: B- or Soret-band at about 350-500 nm, generally with molar absorbance of 10^5 $M^{-1}cm^{-1}$, and Q-bands at 500-750 nm with usually one order of magnitude lower intensities. The bands in the ultraviolet region (in the order of decreasing wavelength: N, L, M) are more diffuse and have smaller molar extinction coefficients [81]. However, the Q- bands of the free-base ligands split as a result of the presence of protons on two diagonally situated pyrrolic nitrogens (Fig. 1), more exactly as a result of the reduced symmetry (because of the disappearance of the fourfold rotation axis) compared to the deprotonated or metallated form. This split is not detectable in the Soret-region, therefore the two types of bands in the visible region are very different. Sofar this experimental phenomenon could not be correctly explained by quantum chemical calculations [78, 82]. The simple 4 MO model of Gouterman has not proved to be suitable either in this respect [83]. (Notwithstanding, most of the experimental chemists try to theoretically interpret their experiences by the application of this simplified approximation.)

As a consequence of the difference between the two absorption bands in the visible region, the fluorescences originating from the two different excited states (first singlet or singlet-1 excited state occupied by Q-excitation, second singlet or singlet-2 state by Soret-absorption) significantly vary.

In the UV-Vis spectra the vibronic origins and overtones (mainly the skeleton vibration [84]) superpose on the electronic excitation, therefore the bands are used to be designated with the following symbols: B or Q(x,y), where "x" is the vibrational quantum number in the electronically excited state (singlet-1 in Q-absorption, singlet-2 in Soret-absorption), "y" is that in the electronic ground state [85]. Under normal conditions, absorption, excitation starts from the lowest vibronic state (vibrational quantum number y=0) in the electronic ground state as well as the luminescence from lowest vibronic state (x=0) in the electronically excited state.

3.1. Soret-absorption

Table 1. Wavelength and molar absorbance of the B(0,0) band in the investigated TSPP compounds with the ionic radius of the metal center.

type of porphyrin	complex	ionic radius /pm [86]	B(0,0) /nm	ε {B(0,0)} /10^5 $M^{-1}cm^{-1}$	ref.
in-plane metallo-porphyrin	$Al^{III}TSPP^{3-}$	53.5	403	2.04	[19]
	$Fe^{III}TSPP^{3-}$	60	393	1.26	[73, 75]
	high-spin $Mn^{III}TSPP^{3-}$	64.5	400	2.05	[20]
	$Cu^{II}TSPP^{4-}$	73	412	4.72	-
	$Au^{III}TSPP^{3-}$	85	405	2.25	[77]
	$Pd^{II}TSPP^{4-}$	86	412	3.42	[20]
free base	H_2TSPP^{4-}	-	413	4.66	[87]
protonated free base	H_4TSPP^{2-}	-	436	6.08	-
	$(H_4TSPP^{2-})_2$	-	491	4.15	-
border-line case metallo-porphyrin	$Zn^{II}TSPP^{4-}$	74	421	6.40	-
	$Fe^{II}TSPP^{4-}$	78	421	4.48	[73, 75]
	$Mn^{II}TSPP^{4-}$	83	421	4.48	[20]
	$Ag^{II}TSPP^{4-}$	94	420	2.99	[77]

out-of-plane (OOP) metallo-monoporphyrin	$Cd^{II}TSPP^{4-}$	95	421	5.62	[10]
	$Hg^{II}TSPP^{4-}$	102	421	5.62	[22, 71]
	$Bi^{III}TSPP^{3-}$	103	421	6.44	[78]
	$Ln^{III}TSPP^{3-}$	86 – 103	~ 421	~ 5	[79]
	$Ag^{I}_2TSPP^{4-}$	115	421	2.92	[77]
	$(Hg^{I}_2)_2TSPP^{2-}$	119	421	5.60	[76]
	$Tl^{I}_2TSPP^{4-}$	150	421	6.31	[72]
axially ligated OOP metallo-monoporphyrin	$(Cl)Tl^{III}TSPP^{4-}$	88.5	428	5.73	[74]
	$(HO)Cd^{II}TSPP^{5-}$	95	431	5.02	[10]
OOP metallo-bisporphyrin	$Ln^{III}_x(TSPP)_2^{3x-12}$ *	86 – 103	~ 423	~ 5	[79]
	$Hg^{II}_2(TSPP)_2^{8-}$	102	422	4.91	[22]
	$Hg^{II}_3(TSPP)_2^{6-}$	102	433	5.37	[22]
	$(Hg^{I}_2)_2(TSPP)_2^{8-}$	119	426	5.74	[76]
more distorted metallo-porphyrin	low-spin $Mn^{III}TSPP^{3-}$	58	467	2.78	[20]
	i-$Bi^{III}TSPP^{3-}$	103	466	2.63	[78]
	$Pb^{II}TSPP^{4-}$	119	464	3.44	[79]
distorted free base	$H_2TSPPBr_8^{4-}$	-	476	1.99	[10, 88]

* x=1-3, depending on the lanthanide(III) and the circumstances

On the basis of the molar extinction coefficient of the free-base porphyrin at the Soret-band (Table 1) and the Bouguer-Lambert-Beer law, if 0.01 change in the absorbance can be precisely measured in a 1 cm optical path length, 2.15×10^{-8} M change in the concentration can be detected. If the spectrophotometer is more precise or the path length can be longer, this concentration (limit of detection) may be smaller.

Porphyrins are strong bases, and their third and fourth protonation steps hinder the potential coordination of metal ions; for the H_2TSPP^{4-} $pK_3 = 4.99$, $pK_4 = 4.76$ [80]. Upon protonation, the Soret-band of the free base shifts toward higher wavelengths as a consequence of the repulsion of the four protons in the coordination cavity, together with the saddle distortion of the periphery, and the twisting of the phenyl rings from almost perpendicular orientation closer to the porphyrin plane (Fig. 4). Similarly large redshifts can be observed in the case of metalloporphyrins, hence, not only the hindrance of complex formation can occur, rather the redshifted spectra can be misinterpreted in an analytical determination (based only on the Soret-absorption) without adjusting the pH above the pK_3+0.5 value. The potential (head-to-tail or head-to-head) dimerisation, aggregation of protonated porphyrins [12] {forming $(H_4TSPP^{2-})_2$ in Table 1} at higher concentration and ionic strength can cause further misapprehension due to the larger redshift {and (half)width} of the absorption bands as a result of the strong π–π (or stacking) interactions between the macrocycles.

Bis- (or oligo-) porphyrins (so called sandwich structures) can also be formed in the case of dome-distorted, out-of-plane metalloporphyrins: an out-of-plane metal center can simultaneously coordinate two macrocycles {e.g. in $Ln^{III}(TSPP)_2^{9-}$}, as well as two metal ions can connect to one ligand {e.g. in $Tl^{I}_2TSPP^{4-}$ or $Hg^{II}_3(TSPP)_2^{6-}$}. In these bisporphyrins the π–π interactions through the metal center can be weaker than in the (head-to-tail) protonated aggregate. Hence, the spectral changes are smaller {e.g. in $Hg^{II}_3(TSPP)_2^{6-}$ or $Hg^{II}_2(TSPP)_2^{8-}$ compared to $Hg^{II}TSPP^{4-}$}. This difference can originate from the smaller overall distortion of the macrocycle, together with the smaller twisting of the phenyl groups.

H_2TSPP^{4-} is a so strong base that it can not deprotonate in water, only in an 80:20=DMSO:water solvent mixture: $p\beta_2$=32,80±0,04 [89], and $pK_1 \approx pK_2 \approx 16$ [85]. (At pH≈16 the free-base and the deprotonated porphyrin would be present in 1:1 ratio.) The wavelength of B(0,0) band of the deprotonated form, $TSPP^{6-}$, {ε(439 nm)=4.88×10^5 $M^{-1}cm^{-1}$} is located between that of the free-base H_2TSPP^{4-} {ε(419 nm)=4.91×10^5 $M^{-1}cm^{-1}$} and the protonated porphyrin H_4TSPP^{2-} {ε(445 nm)=3.98×10^5 $M^{-1}cm^{-1}$}. Furthermore, it is close to that of the $Zn^{II}TSPP^{4-}$ {ε(426 nm)=5.71×10^5 $M^{-1}cm^{-1}$}, and further from that of $Cu^{II}TSPP^{4-}$ {ε(418 nm)=4.10×10^5 $M^{-1}cm^{-1}$} in this solvent mixture [89]. The redshift of the deprotonated ligand's band compared to that of the free base originates from the extension of delocalization by the lone electron pairs of the two deprotonated pyrrolic nitrogens. The cavity of this structure serves as a real coordination sphere for the metal center, therefore the spectral effect of the metalation should be related to the properties of this deprotonated porphyrin. However, in water we are not able to exactly make such a comparison, we can only learn from these experimental results the following: the Soret-bands of the investigated out-of-plane metallo-monoporphyrins are very similar to those of the mentioned border-line cases in water (Table 1). Furthermore, the absorption spectra of the latter ones (beside Zn^{2+}, Mg^{2+} was also studied) are close to that of the deprotonated ligand in DMSO:water mixture. Consequently, in the typical out-of-plane complexes and in those of border-line cases with ionic metal-nitrogen bonds (after Barnes and Dorough [26]), the atomic orbitals of the metal ion do not considerably perturb the molecular orbitals of the porphyrin. Therefore it has insignificant electronic effect on the $\pi\pi^*$ transitions of the deprotonated ligand, and it influences those of the free-base ligand only through the deprotonation. The dome distortion in the out-of-plane complexes would have only a slight steric impact. These phenomena result in the common, so-called OOP or SAT character (OOP=out-of-plane or SAT=sitting-atop) in the spectral properties [22, 74].

The typical in-plane metalloporphyrins show blueshifts in the Soret-range compared to the deprotonated ($Cu^{II}TSPP^{4-}$ in DMSO:water) as well as to the free-base porphyrin because the atomic orbitals of their metal center covalently bonded in the plane can overlap more strongly with the occupied molecular orbitals (the highest in energy is the HOMO) of the ligand, resulting in a stronger reduction in energy; while the unoccupied MOs (the lowest is the LUMO) do not change. Accordingly, the energy gaps between the excited and ground states increase (Scheme 1), i.e. the wavelengths of $\pi\pi^*$ (intraligand) electronic transitions decrease compared to the free-base (Fig. 6) as well as to the deprotonated porphyrin. In the out-of-plane complexes, the atomic orbitals of the more weakly bonded metal ions may slightly influence the unoccupied MOs and lesser the occupied ones, resulting in the decrease of the energy gaps, i.e. the increase of the corresponding wavelengths. If the bands of the different types of complexes could be compared to the deprotonated ligand, a small blueshift would be observed for the common out-of-plane metalloporphyrins, and larger blueshifts for the in-plane, planar complexes. Among the latter ones the differences are slightly higher (Table 1) as a consequence of the different electron configurations of metal ions.

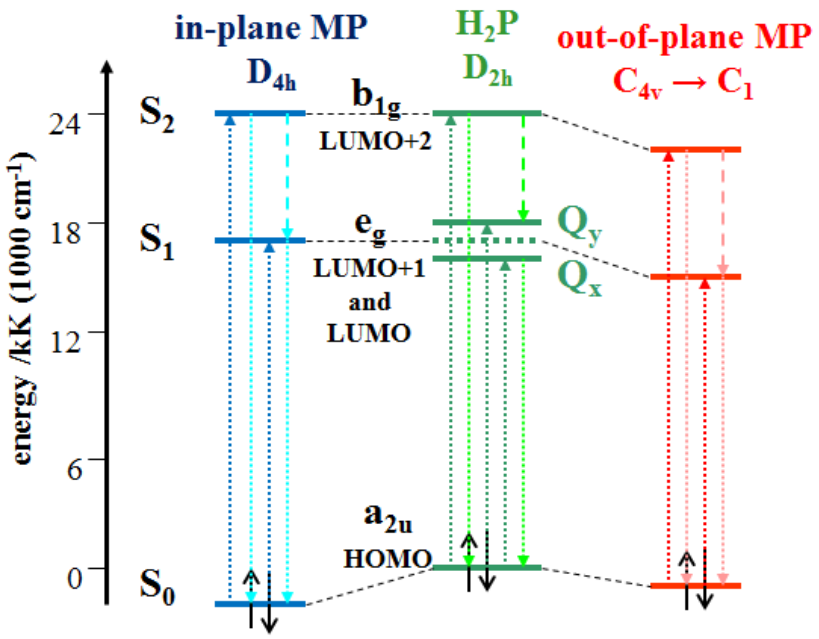

Scheme 1. Simplified energy level diagram for the change of the porphyrin's molecular orbitals (responsible for the Soret- and Q-absorption; their represented symmetries are valid for the ideal D_{4h} structure) in the different types of complexes [19].

In a spectrophotometric detection method of metal ions by porphyrins (or by other ringed, chelate ligands) based on the measurement of the Soret-absorption, we must presume on a lot of interferences: the metal ions possessing a size above or around the critical value compared to the cavity of the ligand will have similar, almost the same absorption properties. Additionally, the metal ions under the critical radius (or having a critical size, but preferring square planar coordination) will have slightly different spectral data, however, not too far from those of the free base (see, e.g. $Cu^{II}TSPP^{4-}$ in Table 1).

The $\pi\pi^*$ (intraligand) electronic transitions will be more significantly changed if the coordination of metal ion results in a considerable structural modification of the macrocycle too. We applied the octabrominated free-base ligand ($H_2TSPPBr_8^{4-}$) to demonstrate the spectral effect of the extreme saddle distortion (Table 1 and Fig. 6).

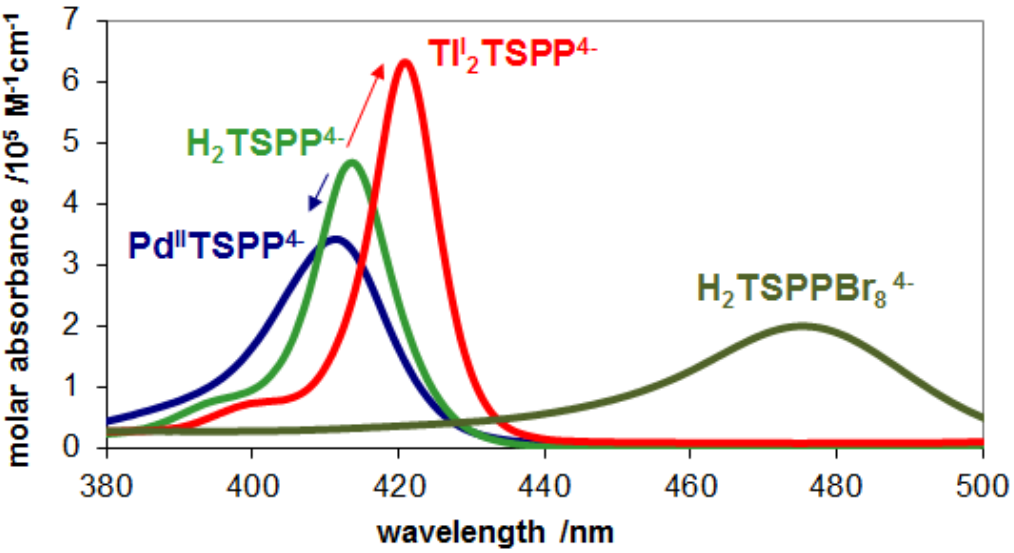

Fig. 6. Absorption spectrum of the free-base (H_2TSPP^{4-}), the highly distorted free-base ligand ($H_2TSPPBr_8^{4-}$), a typical in-plane ($Pd^{II}TSPP^{4-}$) and a typical out-of-plane metalloporphyrin ($Tl^{I}_2TSPP^{4-}$) in the Soret-range.

Lead(II) ion possesses one of the highest out-of-plane distance (i.e. the distance between the metal ion and the plane of four pyrrolic nitrogens) measured: 117 pm in its tetrapropyl-porphyrin complex [90]. Therefore its complex is very labile, besides it belongs to the most highly dome-distorted structures (called as roof in [90]). Also a ruffled-like deformation of the periphery superposes on this high doming, which results in a large redshift, called also as bathochromic or (not quite correctly) hyperchromic effect (bathochromic effect means the increase of the wavelength, while hyperchromic effect means the increase of the absorbance or molar extinction coefficient). Considering the spectral effects, the complexes possessing so highly redshifted absorption bands were named by Gouterman as hyper-porphyrins [25]. According to his definition, this category involves the complexes, whose absorption spectra can not be described with his 4 MO model [83]. (Nevertheless, the Soret-bands of porphyrins can not be usually described with the 4 frontier MOs [78, 82].)
Depending on the highest occupied electron subshell of the metal center (i.e. its field, p- or d-, in the periodic table) he made subcategories: among our results in Table 1. $Pb^{II}TSPP^{4-}$ and i-$Bi^{III}TSPP^{3-}$ would be p-type, and low-spin $Mn^{III}TSPP^{3-}$ d-type hyper-porphyrin.
In this categorization of metalloporphyrins, Gouterman did not take the steric (distorting) effects into consideration, only the electronic effects of metal ion (through its electron configuration). Therefore he had to slightly modify his aspect on the basis of his own experiences with metal-free, more exactly protonated porphyrins, which showed hyper-porphyrin character too [91]. The real origin of these large redshifts is the highly distorted structure. Hence, the principle of Gouterman's categorization is obsolete and its applicability is limited.

3.2. Equilibrium and kinetics of the complex formation

Our further experimental proof against this categorization of metalloporphyrins is that "hyper-porphyrins" can appear as intermediate (with shorter or longer lifetime depending on the metal ion) during the formation of simple out-of-plane metallo-monoporphyrins. Furthermore, the absorption spectra of these intermediates in water are very similar to those of the end-product of metalation in hydrophobic systems in the case of "typical p-type hyperpophyrins", namely if the electron configuration of metal ion is ns^2np^0, e.g. thallium(I), lead(II), and bismuth(III), and also silver(I) without s-electrons. The amount of this thallium(I) [72] {and silver(I) [77]} intermediate complex in water is negligible, in the case of bismuth(III) is considerable [78] (therefore the intermediate, i-$Bi^{III}TSPP^{3-}$can be spectrophotometrically studied, see in Table 1 and Table 3), however, in the case of lead(II) is dominant because its transformation reaction is very slow (but it can be enhanced, e.g. by photolysis [79]). The absorption spectrum of the end-product of these transformation reactions is very similar to those of the common out-of-plane metallo-monoporphyrins. This phenomenon may be attributed to the appreciable coordination ability or the polarizing effect of water molecules, which can promote the complex to overcome the kinetic energy barrier toward the more stable structure, in which the metal center is located closer to the ligand plane, resulting in the decrease of distortion, as well as that of the redshift.
As mentioned in Section 1.2 (*Distortion of porphyrins*), the too short metal-nitrogen bonds through the contraction of the coordination cavity can result in ruffled or saddle deformation as well as in a large redshift of absorption band. However, in the case of typical examples, namely nickel(II) [4, 13], chromium(III) [14, 15], and manganese(III) porphyrins [17] (in Table 1), the

low-spin and ruffled complex can be in a spin isomerisation equilibrium with the high-spin and planar form. This reaction can be influenced by the strength of M-N bonds (which can be modified due to the electronic effects of peripheral or axial substituents), due to the size of the coordination cavity (which can be decreased due to the saturation of methylidine bridges or can be increased due to the saturation of π bonds between β carbons [4], or can be drastically changed by the replacement of the methylidine bridge(s), e.g. by direct bond(s) between the α carbons [4, 92] or by aza bridge(s) [93]).

We can learn from these examples of metalloporphyrins possessing highly redshifted absorption that several metal ions can form different complexes, depending on the porphyrin, potential axial ligands as well as the solvent too. Moreover, in the case of out-of-plane metalloporphyrins, sandwich complexes (with e.g. metal:porphyrin 1:2, 2:2, 3:2 compositions, see in Table 1) can also be formed. This can cause mistakes in a spectrophotometric detection method of metal ions if the analyst is not circumspect enough.

The formation of metalloporphyrins in aqueous solution (or in other polar solvents) is an equilibrium reaction, owing to the higher activity and mobility of metal ions than in nonpolar solvents [94]. However, the insertion of a smaller metal ion, which could form an in-plane complex, as well as its dissociation from the cavity may be kinetically hindered due to the rigidity of the porphyrin ligand. Therefore, the reaction seems to be not a real equilibrium process. An increase of the metal ion concentration may be ineffective in this respect; it can not enhance the complex formation at room temperature. An enhancement of the temperature could be effective, but not in an analytical detection method of metal ions. This problem may be solved by the addition of a small amount of larger metal ion (e.g. Pb^{2+}, Hg^{2+}, Cd^{2+}) to the solution of the smaller one because the insertion of the larger metal ion into the cavity is orders of magnitude faster, however, the stability of its out-of-plane complex is much more lower than that of the in-plane complex of the smaller metal ion. In an out-of-plane metalloporphyrin the dome distortion makes two diagonal pyrrolic nitrogens more accessible from the other side of the ligand, hence, the metal center can be easily exchanged by a smaller one [19, 94]. (That was the basis of the metalloporphyrins' categorization after Barnes and Dorough [26]).

The equilibrial character of the complex formation reaction can be weakened, i.e., the metalloporphyrin formed becomes kinetically more inert, because the porphyrin ligands can stabilize the (even extremely) high oxidation states of metal ions on the basis of their high partial negative charge and polarizing effect: e.g. manganese(III–V) [95], iron(III–V) [96], cobalt (III–IV) [97], molybdenum(V) [98], silver(II–III) [77, 99] are possible oxidation states in porphyrins. (These effects of the macrocycle can be further increased by peripheral substitutions with electron donating groups [85].) Most of these ions do not exist in aqueous solution, only in the coordination cavity of the macrocycle, or even if it can exist, it is not able to insert into the porphyrin because of its small size, as well as its potential, stabilizing (e.g. oxo) ligands. However, their complexes can form spontaneously in the reaction between their lower oxidation state (also larger size) ions and the porphyrin, e.g. Fe^{2+}, Mn^{2+}, Co^{2+} can insert into the cavity of the macrocycle, where they are oxidized to their trivalent state by the pyrrolic protons [19, 20] (Eq. 1.).

$$H_2P + Mn^{2+} \leftrightarrow Mn^{II}P + 2\,H^+ \rightarrow Mn^{III}P^+ + \frac{1}{2}H_2 + H^+ \qquad (1)$$

On the other hand, silver(I), gold(I), and e.g. mercury(I) ions may undergo disproportionation in the coordination cavity of the ligand [20, 77, 99] (Eq. 2).

$$H_2P + Ag^+ \leftrightarrow Ag^IP^- \,(+2\,H^+) \xleftrightarrow{Ag^+} Ag^I_2P \rightarrow Ag^{II}P + Ag^0 \qquad (2)$$

In an analytical detection method of metal ions, these redox reactions (spontaneous oxidation or disproportion) inside the metalloporphyrins result in that the analytical, calibration curve for metal ion concentrations will be nonlinear, it may have even breakpoint(s) [77]. Moreover,

nonlinear, but continuous analytical curves (polynomial functions) appear in every case if the composition of metalloporphyrin is not 1:1 (metal:ligand) (Table 1). Beside the bisporphyrins already mentioned, dinuclear out-of-plane monoporphyrins (2:1 complexes) are fairly frequent if the metal ion has one positive charge and large size, i.e. its charge density is low enough, e.g. in the case of lithium(I) [100], thallium(I) [72], mercury(I) [76] and silver(I) ions [77].
We investigated the complex formation from equilibrial and kinetic aspects too, because: "the metalloporphyrin formation reaction is one of the important processes from both analytical and bioinorganic points of view" [29]. On the basis of our results, the concentration of the metal ion can be estimated on the basis of Eqs. 3-4, using spectrophotometric data. (Proton concentration is adjusted by buffer, therefore it may be included in the apparent stability contant $\beta'_{x:y}$.)

$$x\,M^{z+} + y\,H_2TSPP^{4-} \Leftrightarrow M_x(TSPP)_y^{xz-6y} + 2y\,H^+ \qquad (3)$$

$$\beta'_{x:y} = \frac{\beta_{x:y}}{[H^+]^{2y}} = \frac{[M_x(TSPP)_y^{xz-6y}]}{[M^{z+}]^x[H_2TSPP^{4-}]^y} \qquad (4)$$

From the Soret-absorption of the free-base porphyrin (Table 1), 2.15×10^{-8} M limit concentration change was calculated to be reliably measured. For this purpose a 10 % conversion is required in an equilibrial reaction, hence, the initial free-base concentration should be $c(H_2TSPP^{4-}) = 2.15\times10^{-7}$ M. The ratio between the complex, $[M_xTSPP^{xz-6}]$, and the actual free-base concentration, $[H_2TSPP^{4-}]$, in the case of a metallo-monoporphyrin (y=1) in Eq. 4 will be 1:9. Thereafter, the excess or actual concentration, $[M^{z+}]$, and the initial concentration of the metal ion, $c(M^{z+})$ (or it can be called as the limit of detection=LoD by this method for Table 2), are resulted from Eq. 5. (At such a low free-base concentration, the measure of bisporphyrins' formation is negligible [22, 76].)

$$[M^{z+}] = \sqrt[x]{\frac{1}{9\times\beta'_{x:1}}} \quad\Rightarrow\quad c(M^{z+}) = x\times[M_xTSPP^{xz-6}] + [M^{z+}] \qquad (5)$$

Also the time (t) required for the complexation (or it can be called as the time for detectability, or simply the time of detection=ToD by this method for Table 2) in this ratio (conversion) and until these concentrations can be estimated by Eq. 6, which is the analytical formula for an overall second order reaction (first order for both reagents). This approximation is very simplified because it does not take the backward reaction into account, the dissociation of the complex, therefore the supposed time will be under estimated.

$$k_+ t = \frac{1}{c(M^{z+}) - c(H_2TSPP^{4-})} \ln \frac{c(H_2TSPP^{4-})\left(c(M^{z+}) - \{M_x(TSPP)_y^{xz-6y}\}\right)}{c(M^{z+})\left(c(H_2TSPP^{4-}) - \{M_x(TSPP)_y^{xz-6y}\}\right)} \qquad (6)$$

Table 2. Apparent stability and formation rate contants of the investigated metallo-TSPP complexes with the estimated limit (LoD) and "time" of detection (ToD) of metal ions.

complex	ionic radius /pm	$\lg\beta'_{x:y}$ /M^{1-x-y}	LoD /M	k_+ /$M^{-1}s^{-1}$	ToD /min
$Al^{III}TSPP^{3-}$	53.5	5.6	3.3×10^{-7}	0.4	15300
$Zn^{II}TSPP^{4-}$	74	~4.2	$\sim7.4\times10^{-6}$	~1.5	~160
$Fe^{II}TSPP^{4-}$	78	4.4	4.9×10^{-6}	2.5	140
$Cd^{II}TSPP^{4-}$	95	5.9	1.8×10^{-7}	320	33
$Hg^{II}TSPP^{4-}$	102	6.0	1.5×10^{-7}	790	17
$Bi^{III}TSPP^{3-}$	103	4.0	1.1×10^{-5}	25	6.2
$(Hg^{I}_2)_2TSPP^{2-}$	119	10.1	3.2×10^{-6}	~40	~13
$Tl^{I}_2TSPP^{4-}$	150	3.6	5.6×10^{-3}	$\sim4\times10^{-4}$	$\sim1\times10^{5}$
$(Cl)Tl^{III}TSPP^{4-}$	88.5	7.0	3.3×10^{-8}	270	320

$(HO)Cd^{II}TSPP^{5-}$	95	6.9	3.5×10^{-8}	3600	21
$(HO)Cd^{II}TSPPBr_8^{5-}$	95	7.4	2.6×10^{-8}	6.6×10^{4}	2.1
$Pb^{II}TSPP^{4-}$	119	5.5	3.5×10^{-7}	120	42

We studied the formation of only the aluminium(III) complex among the in-plane metalloporphyrins from equilibrial and kinetic aspects because it is a real equilibrium reaction, contrary to the complexation of other smaller metal ions, e.g. iron(III) and manganese(III) (Table 1). The insertion of some larger-size, but coplanarly coordinated metal ions (e.g. Cu^{2+}, Pd^{2+}, Au^{3+}) is also an equilibrial process, the examination of which is in progress [79]. The (apparent) stability constants ($\beta'_{x:y}$) of these in-plane metalloporphyrins are not much higher, but their formation rate constants (k_+) are, in general, significantly lower than those of the out-of-plane metalloporphyrins (Table 2). Consequently, the estimated concentration limits are not much lower, but the estimated "times of detection" at these limit concentrations are significantly higher. The main exception among the investigated out-of-plane metalloporphyrins is the complex of the extremely large thallium(I) ion with the lowest stability and highest LoD, moreover the slowest formation and longer ToD, as well as one of the highest lability. The lability is proportional with the dissociation rate constant (k_-) of complexes, which value can be calculated as the ratio of the formation rate and the apparent stability contants from Table 2. The main difference between in-plane and out-of-plane (together with border-line case) complexes appears in their kinetic parameter: it is around 10^{-6} s^{-1} in the case of in-plane metalloporphyrins, however, ~10^{-4} s^{-1} for OOP ones and border-line case. The lability and the instability of the complexes are proportional with the radius of the metal ions among the OOP and border-line case metallo-monoporphyrins (in the same composition: 1:1 or 2:1). This phenomenon is the obvious consequence of the coincident change of the out-of-plane distance and the radius; on the other hand, this is the reason of the increasing exchangeability of the metal center, leading to the mentioned categorization of metalloporphyrins by Barnes and Dorough [26].

The under-estimated ToD values in Table 2 (in minute unit!) seem to be already extremely high for a routine analytical method at the given LoDs. Certainly, they can be improved by higher reactant concentrations, but only at the expense of LoDs. However, on the basis of investigation of the complex formation mechanism [29], we can suggest techniques for the simultaneous decrease of both analytical parameters, i.e. increase of stability and formation rate constant. One of the simplest methods is the application of a potential axial ligand (in a suitable concentration), which can coordinate to the metal ion in the solution, before the addition of porphyrin, and it can shape an asymmetric coordination sphere around the metal ion due to the formation of a complex with an odd coordination number, mainly 1 or 3 (without the solvent molecules) [101]. In this asymmetric structure, the applied ligand, owing to its trans effect, enhances the solvent molecule (e.g. water) exchange reaction in the opposite coordination position. That can highly accelerate the metal ion insertion into the coordination cavity of porphyrin, i.e. it can increase the formation rate constant of metalloporphyrins by orders of magnitude. If the applied ligand remains on the metal center (this is not evident) in axial position compared to the porphyrin, it can strengthen the bonds between the metal ion and the pyrrolic nitrogens, owing to its trans effect as well, i.e. it can also increase the stability constant of the metalloporphyrin. Hence, it can decrease simultaneously both the LoD and ToD, or, if it does not remain on the metal center, only the ToD. For such an application, even a simple Lewis base as hydroxide may be efficient, at a corresponding pH, forming mono- or trihydroxo complex: we used the former one in the case of cadmium(II) [10], while the latter one in the case of lead(II) [79]. The effects of one OH^- at pH=8 for the formation of cadmium(II) TSPP are presented in Table 2: the formation rate, as well as the apparent stability constant are increased for about 11-fold, while the LoD is decreased by ~5-fold, and the ToD by ~1.6-fold.

Another simple, but more laborious method was already described in more details in Section 1.2 (*Distortion of porphyrins*): the porphyrin ligand must be distorted, e.g. by overcrowded substitution on the periphery, decreasing its basicity and increasing the coordinative abilities toward metal ions (, as well as the affinity of metal center to axial ligands) [3]. The octabromination of H_2TSPP^{4-} results in a further ~3-fold increase of the stability contant, together with a 1.4-fold decrease of LoD, but a ~19-fold growth of the formation rate contant, as well as a 10-fold decrease of ToD in the case of the above mentioned complexation of monohydroxo cadmium(II) {$(HO)Cd^{II}TSPP^{5-}$ compared to $(HO)Cd^{II}TSPPBr_8^{5-}$ in Table 2} [10].

The potential in the axial coordination can be observed from the other direction too: metalloporphyrins may be applied in an analytical procedure to detect a molecule, which has a Lewis base-type group with a lone electron pair, it can be coordinated to the metal center in axial position. The coordination of the first axial ligand results usually in the pull of the metal center further from the coordination cavity, together with the appearance or increase of dome distortion as well as the redshift of the absorption band [21]; in our experiments $(HO)Cd^{II}TSPP^{5-}$ compared to $Cd^{II}TSPP^{4-}$ in Table 1. The redshift originating from the axial coordination (, as well as the stability constant of the axially ligated complex owing to the mentioned trans effect) is in linear correlation with the electron donor properties (Drago parameter) of the axial ligand [102].

However, the coordination of the first axial ligand to a highly distorted, redshifted ("hyper") metalloporphyrin can cause special effects: the highest measured out-of-plane distances in "p-type hyper" metalloporphyrins may be decreased due to the axial coordination [103, 104], together with the reduction of the redshift compared to the free-base ligand. In quantum chemical calculations we tried to study the theoretical limit of the dome distortion, the domedness, and we found that the value of this parameter increases to a 55 pm together, but nonlinearly, with the out-of-plane distance {to 130 pm in $(HO)La^{III}P$, where P=unsubstituted porphin}, above this limit the further growth of OOP distance reduces the domedness, as well as the redshift, e.g. in $Tl^{I}P^{-}$ the OOP distance is 150 pm, the domedness 45 pm, while in $(HO)Tl^{I}P^{2-}$ 201 pm and 37 pm, respectively [79]. Moreover, in the metalloporphyrins with cavity contracted by the too short M-N bonds ("d-type hyperporphyrins"), the coordination of the first axial ligand pulls out the metal center from this contracted cavity. Therefore, the length of the M-N bonds (and probably the spin multicipity) increases, the ruffled (or saddle), as well as the overall distortion decreases, together with the large redshift, e.g. in the reaction between $Cr^{III}TSPP^{3-}$ and hydroxide [105].

If the investigated molecule as potential axial ligand is a bulky group, it sterically hinders the axial coordination of other ligands to the metal center from the same side of the porphyrin plane. However, from the opposite side of the porphyrin the second axial ligand can connect to the metal ion, pulling it back towards the coplanar position (and probably setting back the position of absorption band close to that of the initial complex without axial ligands), only in the case if the complex is a typical in-plane one. Since, already in a border-line case complex the first axial coordination results in such a large out-of-plane distance (because of the ionic character of the M-N bonds), that the second axial ligand from the opposite side from the porphyrin is not able to coordinate to the metal ion across the coordination cavity [102].

Consequently, in a spectrophotometric detection method of Lewis bases as potential axial ligands, a border-line case or an out-of-plane metalloporphyrin may be more suitable if the molecule can form 2:1 (axial ligand:porphyrin) complex with the in-plane metalloporphyrins, and this compound has almost the same absorption spectrum as the initial metalloporphyrins. Certainly, the metalloporphyrin has to be chosen for the determining molecule on the basis of its Pearson hard-soft character.

3.3. Q-absorption

Other absorption bands of porphyrins in the visible region of electromagnetic spectrum, beside the B- or Soret-, are the Q-bands. They split in the free-base ligands (Scheme 1) as a result of the disappearance of the fourfold rotation axis because of the diagonally situated pyrrolic protons. Hence, five bands can be observed in the Q-region originating from the superposition of skeleton vibrations on two, split electron excited states (Q_x and Q_y) (Fig. 8). However, the fourfold-axis symmetry, together with the degeneration of singlet-1 excited state is restored by deprotonation ($TSPP^{6-}$), metalation, as well as by the protonation (H_4TSPP^{2-}). In this latter case, in the slightly saddle-distorted structure, a fourfold inversion axis appears similarly as in ruffled deformed metalloporphyrins (Fig. 3), resulting also in degeneration. (Only twofold axis can be found in the wave distorted complexes, therefore their Q-bands may be split too.) If the singlet-1 state is degenerate, only 3 absorption bands can be observed (e.g. $Tl^{I}_2TSPP^{4-}$ in Fig. 7, the others are truncated under 500 nm).

Consequently, the shifts of Q-bands of free-base porphyrins upon their reactions must be calculated from the average energy of their $Q_x(0,0)$ and $Q_y(0,0)$ bands [83]. It means 589 nm in the case of H_2TSPP^{4-} (Fig. 7).

Table 3. Wavelength and molar absorbance of the Q(0,0) band in the investigated TSPP compounds.

complex	Q(0,0) /nm	ε {Q(0,0)} /10^3 $M^{-1}cm^{-1}$	ref.
$Al^{III}TSPP^{3-}$	y 561 x 653	13.58 4.38	[19]
$Fe^{III}TSPP^{3-}$	529	11.29	[73, 75]
high-spin $Mn^{III}TSPP^{3-}$	~540	~15	-
$Cu^{II}TSPP^{4-}$	577	2.94	-
$Au^{III}TSPP^{3-}$	550	3.24	[77]
$Pd^{II}TSPP^{4-}$	553	4.51	[20]
H_2TSPP^{4-}	y 553 x 633	6.99 3.98	[22, 87]
H_4TSPP^{2-}	647	66.12	-
$(H_4TSPP^{2-})_2$	708	259.3	-
$Zn^{II}TSPP^{4-}$	596	8.32	-
$Fe^{II}TSPP^{4-}$	596	8.41	[73, 75]
$Mn^{II}TSPP^{4-}$	~595	~8	-
$Ag^{II}TSPP^{4-}$	568	3.40	[77]
$Cd^{II}TSPP^{4-}$	596	9.24	[10]
$Hg^{II}TSPP^{4-}$	594	7.69	[22, 71]
$Bi^{III}TSPP^{3-}$	596	9.00	[78]
$Ln^{III}TSPP^{3-}$	~595	~9	[79]
$Ag^{I}_2TSPP^{4-}$	596	5.64	[77]
$(Hg^{I}_2)_2TSPP^{2-}$	594	9.06	[76]
$Tl^{I}_2TSPP^{4-}$	594	9.45	[72]
$(Cl)Tl^{III}TSPP^{4-}$	603	10.84	[74]
$(HO)Cd^{II}TSPP^{5-}$	611	14.28	[10]
$Hg^{II}_2(TSPP)_2^{8-}$	628	15.55	[22]
$Hg^{II}_3(TSPP)_2^{6-}$	628	16.02	[22]

$(Hg^{I}_2)_2(TSPP)_2^{8-}$	619	16.09	[76]
low-spin $Mn^{III}TSPP^{3-}$	596	28.01	[20]
i-$Bi^{III}TSPP^{3-}$	643	18.08	[78]
$Pb^{II}TSPP^{4-}$	656	21.49	[79]
$H_2TSPPBr_8^{4-}$	753	10.18	[10, 88]

The molar extinction coefficients of the Q-bands are usually one order of magnitude lower than those of the Soret-bands, hence, an analytical determination method based on Q-absorption may be less sensitive. The Q(1,0) band is more intense than Q(0,0) for most of the investigated TSPP derivatives, but the latter one will be required for us to be compared with the singlet-1 fluorescences.

Nevertheless, the protonated porphyrins, and mainly their dimers (or aggregates) possess much higher molar absorption (Table 3), as well as more redshifted Q-bands than the corresponding metalloporphyrins. Owing to this phenomenon, also the Q-bands must be recorded, beside the Soret-bands, for their more accurate distinction.

The Q(0,0) band of deprotonated $TSPP^{6-}$ {ε(629 nm)=2.29×10^4 $M^{-1}cm^{-1}$} in DMSO:water=80:20 solvent mixture is located between that of the free-base H_2TSPP^{4-} {Q_y(0,0) ε(550 nm)=9.5×10^3 $M^{-1}cm^{-1}$ and Q_x(0,0) ε(645 nm)=5.1×10^3 $M^{-1}cm^{-1}$, their average in energy: 594 nm} and the protonated porphyrin H_4TSPP^{2-} {ε(660 nm)=5.14×10^4 $M^{-1}cm^{-1}$}. Furthermore, it is much closer to that of the border-line case $Zn^{II}TSPP^{4-}$ {ε(599 nm)=1.12×10^4 $M^{-1}cm^{-1}$} than to that of the in-plane $Cu^{II}TSPP^{4-}$ {ε(541 nm)=1.98×10^4 $M^{-1}cm^{-1}$ may be the Q(1,0)} [89]. Namely, the spectral situation is very similar as at the Soret-region was (under the Table 1): the absorption bands of in-plane metalloporphyrins are highly blueshifted compared to that of the deprotonated ligand and lesser blueshifted compared to the average of the split bands of free base. While the Q-bands of OOP and border-line case complexes are lesser blueshifted compared to that of $TSPP^{6-}$, but slightly redshifted compared to the average wavelength of H_2TSPP^{4-} (Fig. 7).

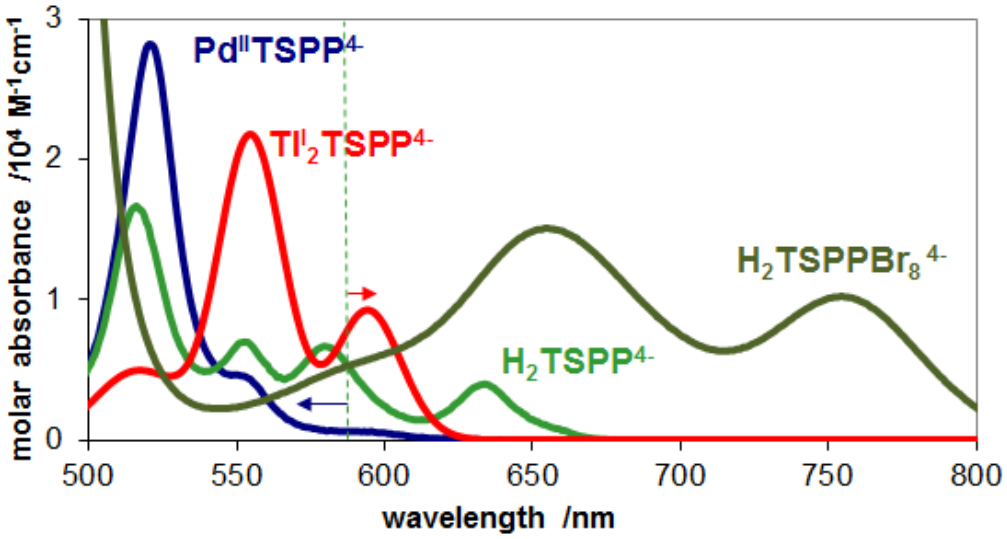

Fig. 7. Absorption spectrum of the free-base (H_2TSPP^{4-}), the highly distorted free-base ligand ($H_2TSPPBr_8^{4-}$), a typical in-plane ($Pd^{II}TSPP^{4-}$) and a typical out-of-plane metalloporphyrin ($Tl^{I}_2TSPP^{4-}$) in the Q-range. The dotted line represents the average energy of Q_y(0,0) and Q_x(0,0) in the free-base ligand (at 589 nm).

The differences between the Q-bands of in-plane metalloporphyrins are more significant, originating from the higher perturbations of their atomic orbitals for the MOs of porphyrin, than in OOP complexes. The most altered ones are those of $Al^{III}TSPP^{3-}$, because they are (x-y) split and redshifted compared to those of the free base, not only its average band. The reason for this phenomenon may be a special distortion, e.g. the above mentioned wave distortion. However, in organic solvents the $(Cl)Al^{III}TPP$ or -OEP (octaethylporphyrin) complexes possess 3 Q-bands [106] instead of 5 in water because of the split. This may suggest not a special deformation in water, rather a special coordination of Al^{3+} to, instead of the pyrrolic nitrogens, the sulphonato oxygens. This assumption is not proved yet, but it may be confirmed by the Pearson-type hard character of Al^{3+} and oxygens, moreover by the blueshifted Soret-band, as well as the redshifted and split Q-bands, which are the spectral evidences of the aggregation of free-base porphyrins [107] due to Al^{3+} bridges. The message of these observations to the analysts is that the peripheral subsituents can also coordinate to metal ions [108], therefore, in a detection method, the porphyrin ligand must be carefully chosen for the metal ions.

The out-of-plane metallo-monoporphyrins display "common" properties at the Q-bands too (Table 3), similarly to the case at the Soret-bands, except $Ag^{II}TSPP^{4-}$ with redshifted Q(0,0) band compared to the average band of the free base. The radius (94 pm) of the silver(II) ion [86] is close to the critical region compared to the size of the ligand cavity, i.e. the distance between the diagonally located pyrrolic nitrogens (this is 420 pm in the deprotonated ligand). In our quantum chemical calculations, the circle of border-line case complexes, together with the region of critical radius flared to about 100 pm due to the significant expansion of the coordination cavity to coplanarly incorporate the metal ion [77]. However, only the Q-bands of this silver(II) complex are redshifted among the investigated border-line cases and OOP complexes.

The redshifts of Q-absorptions for the highly distorted metalloporphyrins (low-spin Mn^{3+}, Pb^{2+} and the intermediate type of Bi^{3+}) are not as large as in the octabrominated free base, rather similar to those for the protonated porphyrin. Moreover, these redshifts for the manganese(III) complex is even lesser, similarly to those of the common OOP ones. These differences in the spectral properties between the Soret- and Q-bands confirm the requirement of the measurement of Q-bands, beside the Soret-bands, for the more accurate identification of metal ions in an analytical method if the concentrations (high enough) make it possible. After all, the number of the interferences between the metal ions is not really reduced by the recording of Q-absorptions, mainly not between the metal ions of border-line case and OOP complexes. However, e.g. the $Cu^{II}TSPP^{4-}$ is not distinguishable from the free-base porphyrin on the basis of their Soret-absorption spectra (Table 1), only on the basis of their Q-bands (Table 3).

For the axially ligated OOP metallo-monoporphyrins the redshifts of Q-bands are slightly larger than for the unligated complexes, furthermore, the presence (or remain) of the axial ligand on the metal center is confirmed by the strengthening of the Q(0,0) band compared to Q(1,0), which relation is valid for the fluorescence too [102]. This spectral effect can be utilized in the spectrophotometrical detection of Lewis bases as axial ligand using metalloporphyrins.

The Q-absorption spectrum of $H_2TSPPBr_8^{4-}$ seems to be irregular because it does not show any split in spite of the presence of two protons on pyrroles. However, the (half)widths of the bands are so large that they may be merged [10]. Similar band broadenings are the typical consequences of the formation of bis- or oligoporphyrins, also in the case of the investigated OOP bisporphyrins too [22, 76]. (In some cases also new bands can appear in the Q-region of bisporphyrins' absorption spectra [107].) This spectral evidence can be very useful in a metal ion detection method to prove the formation of complexes with various compositions. Hence, the potential deviation of the analytical curve from linearity becomes to be explained.

3.4. Other absorption bands

In the region of shorter wavelengths in Fig. 6 (displaying mostly Soret-bands), highly redshifted N-bands of the extremely distorted, octabrominated free-base porphyrins can be observed, similarly to the case of the highly distorted metallo-TSPPs (see examples in Table 1). However, beyond the Q-bands of porphyrins, charge transfer (CT, e.g MLCT=from metal to ligand, LMCT=from ligand to metal) bands can be detected mainly for the paramagnetic in-plane complexes ($Fe^{III}TSPP^{3-}$ at 644, 687 nm; high-spin $Mn^{III}TSPP^{3-}$ at 673, 731, 794, 841 nm [79]). Similar bands in the spectra of the paramagnetic, border-line case ($Fe^{II}TSPP^{4-}$ and $Mn^{II}TSPP^{4-}$) or OOP complexes ($Ag^{II}TSPP^{4-}$ and $Ln^{III}TSPP^{3-}$) do not appear as a consequence of the lower perturbation of metal ion's atomic orbitals for the MOs of ligand. This difference between the types of complexes makes the categorization of the investigated metal ion in possible an analytical detection method, but the molar extinction coefficients of CT bands (and also the mentioned N-bands) are about one order of magnitude lower than those of the Q-bands, hence, about two orders of magnitude than those of the Soret-bands. Therefore, the measurement of CT bands (or N-bands) increases the selectivity, but the concentration necessary for their measurability diminishes considerably the sensitivity of an analytical detection method.

3.5. Singlet-1 fluorescence

Porphyrins belong to the most interesting compounds from the aspects of biological significance, as well as photophysical properties [109]. Only a negligible part of excitation energy is lost via heat dissipation from singlet states, because the overall quantum yield of fluorescence and intersystem crossing resulting in formation of triplet states is over 95%, which is the major reason that makes porphyrins efficient in optical sensations and photosensitizations [85]. Owing to their rigidity and aromatic electronic system they possess two type of fluorescence: the relatively rare and weak singlet-2, as well as the strong singlet-1 fluorescence. The latter one in arylated porphyrins shows a fairly unusual peculiarity: its spectrum is antisymmetric to that of the absorption (Fig. 8). In the free-base porphyrins, the emission derives not from a hypothetical average level of split singlet-1 excited states (Scheme 1), but from the energetically lower S_{1x}-state {populated in $Q_x(0,0)$ absorption}. Therefore, the Q_x-absorption bands must be compared to the S_1-bands. One of the possible reasons for this antisymmetry is the extension of delocalization in the S_1-excited state by the twisting of aryl substituents from almost perpendicular orientation to the porphyrin plane to closer to parallel, causing an alternating excited state.

Beside the symmetrical comparison, the energy difference between Q(0,0) and $S_1(0,0)$ bands (Fig. 8) is a very important photophysical parameter: this is the so-called Stokes shift (Table 4), which is proportional with the structural change during the photon absorption, i.e. the excitation.

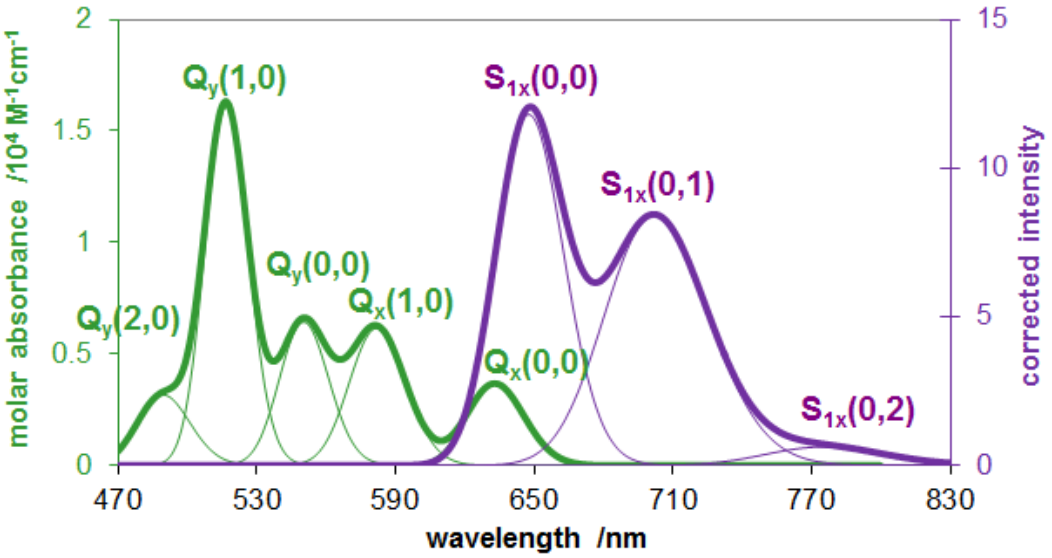

Fig. 8. Singlet-1 fluorescence spectrum of H_2TSPP^{4-} compared to its Q-absorption spectrum.

Table 4. Characteristic S_1-fluorescence data of the investigated TSPP compounds.

complex	$S_1(0,0)$ /nm	S_1-Stokes-shift /cm^{-1}	$\phi(S_1)$ /10^{-2}	ϕ(IC) S_2-S_1	$\tau(S_1)$ /ns	ref.
$Al^{III}TSPP^{3-}$	666	254	0.49	0.49	3.37	[19]
$Pd^{II}TSPP^{4-}$	568	534	0.11	0.22	0.74	-
H_2TSPP^{4-}	648	360	7.53	0.75	10.0	[22]
H_4TSPP^{2-}	674	622	6.19	?	3.9	[12]
$(H_4TSPP^{2-})_2$	717	194	0.061	?	0.10	[12]
$Zn^{II}TSPP^{4-}$	609	400	3.84	0.69	2.70	-
$Fe^{II}TSPP^{4-}$	609	382	0.95	0.74	1.97	[75]
$Ag^{II}TSPP^{4-}$	609	400	0.84	0.21	~0.3	[77]
$Cd^{II}TSPP^{4-}$	609	388	2.59	0.83	3.40	[10]
$Hg^{II}TSPP^{4-}$	609	400	2.39	0.68	2.65	[22, 71]
$Bi^{III}TSPP^{3-}$	609	376	1.94	0.69	3.18	[78]
$Ln^{III}TSPP^{3-}$	~609	~400	~2	~0.65	~3	[79]
$(Hg^{I}_2)_2TSPP^{2-}$	609	396	2.25	0.70	3.71	[76]
$Tl^{I}_2TSPP^{4-}$	609	414	1.90	0.69	3.43	[72]
$(Cl)Tl^{III}TSPP^{4-}$	611	242	0.079	0.28	0.47	[74]
$(HO)Cd^{II}TSPP^{5-}$	629	449	1.02	0.27	0.36	[10]
$H_2TSPPBr_8^{4-}$	828	1170	0.27	0.17	0.15	[10]

An analytical detection method based on S_1-fluorescence measurements may be more sensitive than an absorption technique on the basis of the relatively high emission quantum yields of porphyrins {$\phi(S_1)$ in Table 4} if strong light sources and precise detectors are applied. The spectrofluorometers measure the absolute light intensity emitted by the sample, proportionally with the absorbed light intensity {$I_{abs}=I_0(1-10^{-A})$}, while the spectrophotometers record the transmittance, i.e. the relative difference between the light intensities measured before and after the sample (referred to the previous one, {$(I_0-I_{abs})/I_0$)}, or the absorbance, i.e. the logarithm of the reciprocal value of transmittance. Accordingly, the higher sensitivity derives from the

concept of the devices, not really from the applied porphyrins. Also the quality of the porphyrin using for the fluorescence detection method can influence the selectivity due to its molar (ε), as well as the actual absorption (A). Therefore, the quantum yield of S_1-fluorescences must be determined by excitation at both the Q- {$\phi(S_1)$} and the Soret-absorption bands {$\Phi(S_1\text{-Soret exc})=\phi(\text{IC } S_2\text{-}S_1)\times\phi(S_1)$}. In this way, the ratio of the two data is the quantum yield of the internal conversion between the S_2- and S_1-excited states {ϕ(IC S_2-S_1) in Table 4}. If its value is smaller than the ratio between the absorbed light intensity at Soret-excitation and that at Q-excitation (this depends on the actual absorbances at Soret- and Q-bands, respectively, under the applied concentrations), the Soret-excitation results in higher emitted, S_1-fluorescence light intensity {$I_{em}=I_{abs}\times\phi_{em}$}, as well as higher sensitivity; or if it is smaller, the Q-excitation is more effective. The former case is more feasible at lower porphyrin concentrations, and the latter one at higher concentrations. Moreover, for this decision, also the exact concentration is to be determined, at which the quatum yield of internal conversion is equal with the ratio between the absorbed light intensities at the two types of absorptions: e.g. this concentration is 8.6×10^{-5} M for H_2TSPP^{4-}, but 9.6×10^{-6} M for $(HO)Cd^{II}TSPP^{5-}$ {as a consequence of its much lesser ϕ(IC S_2-S_1)}. On the other hand, the quantum yield of internal conversion between singlet-2 and singlet-1 excited states is proportional with their structural differences, which cause the deviation between the two types of fluorescence.

However, the selectivity is further reduced compared to the absorptions, as a consequence of the blueshifted fluorescence bands of both types (in-plane and out-of-plane) of metalloporphyrins (Fig. 9). The reason of this virtual shift anomaly between absorption and emission in OOP complexes is the above described origin of the S_{1x}-fluorescence in free-base porphyrins. (Since, also their Q-absorption bands would be blueshifted if they would be compared to the split $Q_x(0,0)$ band instead of the Q_y-Q_x average of the free base in Fig. 7 and Table 3).

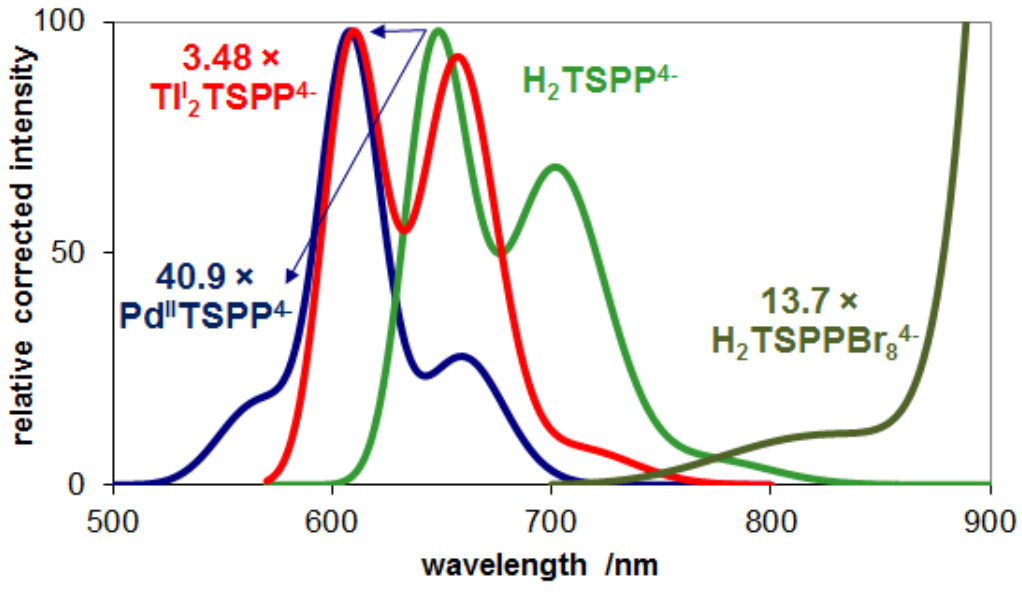

Fig. 9. Singlet-1 fluorescence spectrum of the free-base (H_2TSPP^{4-}), the highly distorted free-base ligand ($H_2TSPPBr_8^{4-}$), a typical in-plane ($Pd^{II}TSPP^{4-}$) and a typical out-of-plane metalloporphyrin ($Tl^{I}_2TSPP^{4-}$).

Furthermore, the circle of detectable metal ions is more limited in the measurement of fluorescences compared to that of absorptions because the highly distorted complexes (Pb^{2+},

low-spin Mn^{3+} and intermediate type of Bi^{3+}), the OOP bisporphyrins and the paramagnetic in-plane complexes (Fe^{3+}, Cu^{2+} and high-spin Mn^{3+}) (the categories see in Table 1) do not luminesce at room temperature. Conversely, the paramagnetic border-line cases (high-spin Fe^{2+} and Mn^{2+}) and out-of-plane complexes (Ag^{2+} and Ln^{3+}) have similar fluorescence properties as the diamagnetic ones (Table 4). Since a paramagnetic metal ion can cause the disappearance of fluorescence by spin-orbit coupling only if it is in the plane. From out-of-plane position it can not so efficiently perturb the molecule orbitals of the macrocycle that results in the common OOP characteristics.

In most of the metalloporphyrins the antisymmetry between the S_1-fluorescence (Fig. 9) and Q-absorption spectra (Fig. 7) decreases compared to the corresponding free-base ligand. Almost all complexes have similarly large Stokes shifts, as well as lifetimes and quantum yields. The few cases with larger decrease of lifetime originate from the heavy-atom-, as electronic effect primarily in the in-plane complexes: $Pd^{II}TSPP^{4-}$ and especially the diamagnetic, but open-shell and non-emitting $Au^{III}TSPP^{3-}$. While in the out-of-plane metalloporphyrins, also the high distortion, as steric effect, can enhance the non-radiative processes: $(Cl)Tl^{III}TSPP^{4-}$, $(HO)Cd^{II}TSPP^{5-}$ and $Ag^{II}TSPP^{4-}$, in which the radii of the metal center are between 88 and 95 pm, i.e., around the upper border of the critical (radius) region (or barely under the ~100 pm value, which originates from our quantum chemical calculation as the new limit [10, 77]). In these three complexes, probably both electronic and steric effets may operate as a consequence of the size of metal centers. From analytical aspect, the determination of the quantum yield of internal conversions between the singlet-2 and singlet-1 excited states may be beneficial because the metal ions can be size-selectively detected, the radii of which are around the upper border of critical region (also Pd^{2+}). Moreover, the procedures for the modification of the cavity size were already described in Section 3.2 (*Equilibrium and kinetics of the complex formation*).

As a luminescence peculiarity in the case of $Pd^{II}TSPP^{4-}$, also phosphorescence appears at room temperature: at $T_1(0,0)$=702 nm, $T_1(0,1)$=756 nm with an about 3.5-fold smaller luminescence quantum yield than its S_1-fluorescence (Table 4). For the demonstration of its S_1-fluorescence spectrum in Fig. 9, the phosphorescence bands were detached by spectrum analysis fitting Gaussian curves to the measured spectrum (similarly as shown in Fig. 8 and Fig. 10). Owing to this peculiarity, the Pd^{2+} ion becomes selectively determinable among the investigated metal ions in this work (Table 1). In the case of other porphyrins (and solvents), the complexes of few further metal ions can phosphoresce also at room temperature, e.g. $Cu^{II}TPP$ [110], $Pt^{II}TMPyP^{4+}$ {TMPyP = meso-tetrakis(1-methyl-4-pyridinium)porphyrin}, $Rh^{III}TtMAPP^{5+}$ {TtMAPP = meso-tetrakis(4-trimethylammonium phenyl)porphyrin} [111].

The phosphorescence bands of $Pd^{II}TSPP^{4-}$ are undoubtedly redshifted (originating from the typical large Stokes shift of phosphorescences) compared to the emission bands of the free-base porphyrin at room temperature, while the other investigated metalloporphyrins possess blueshifted luminescence bands, except $Al^{III}TSPP^{3-}$. This phenomenon may confirm the suspicion describing in Section 3.3 (*Q-absorption*) that Al^{3+} is coordinated by sulphonato oxygens instead of pyrrolic nitrogens because the fluorescence bands of $(Cl)Al^{III}TPP$ are blueshifted compared to those of the corresponding free-base porphyrin [106].

The octabromination of H_2TSPP^{4-} causes large redshift in absorption bands, but even larger in the emission ones as a consequence of the extremely high Stokes shift (Table 4) originating from the highly distorted structure. Hence, this spectrum could not be measured in the range of wavelengths beyond 900 nm because of the detection limit of our equipment (Fig. 9). Therefore, the quantum yield and the lifetime can be only estimated, but these values are much lower than those of the unbrominated free base. In contrast with this highly (saddle) distorted free-base porphyrin, the also highly distorted metalloporphyrins do not luminesce. Accordingly, beside the distortion, as a steric effect, also the coordination of the metal center, as a potential electronic effect, is necessary for the complete quenching of emission. Nevertheless, Wrobel

and coworkers [112] observed fluorescence in the DMSO solution of $Pb^{II}TPP$, but on the basis of Fig. 3 in their publication, its spectrum was the same as that of the free-base porphyrin. In our opinion, this fluorescence originated from the free-base ligand, which could form in a small amount by the dissociation of the labile out-of-plane complex. A similar problematic question, also in an analytical detection method, would and should be answered by the measurement of excitation spectrum, which must usually coincide with the absorption one. In this way, the luminescent species can be identified.
Further difficulties can arise if a strong light source and probably longer excitation times are applied to achieve higher sensitivity in an analytical technique based fluorescence measurement because porphyrins, mainly out-of-plane metalloporphyrins can be photochemically degraded [10, 19, 20, 22, 71-79]. This photoreactivity of $Cd^{II}TSPP^{4-}$ {or exactly $(HO)Cd^{II}TSPP^{5-}$ at pH=8.8} was exploited in a spectrophotometric determination method for Co^{2+} [34].

3.6. Singlet-2 fluorescence

Porphyrins, owing to their rigidity and aromatic system, possess two types of fluorescence: beside the relatively strong S_1-fluorescence in the range of 550–800 nm, a weak luminescence was also observed at 400–550 nm upon excitation at the Soret- (or energetically higher) band. The main requirements of this deviation from Kasha's rule (luminescence occurs in appreciable yield only from the lowest excited state of a given multiplicity) are the structural rigidity and the relatively large energy gap between the singlet-2 and singlet-1 excited states [113]. This latter value is usually about 7000 cm^{-1} in porphyrins. As a consequence of the very low S_2-fluorescence intensity, Raman scattering of the solvent (and also the Rayleigh scattering because of the small Stokes shifts) may disturb the detection, but the scatterings can be easily distinguished from the luminescence because their wavelength changes with that of the excitation. Furthermore, also a careful spectrum analysis (carried out by fitting Gaussian and Lorentzian curves) is recommended for the identification of the detected signals.
The small S_2-fluorescence quantum yields can be, at least partly, attributed to its very short lifetime: several tens of femtoseconds for porphyrins [113] (our equipment is not able for its determination).
In contrast with the antisymmetric spectrum of the singlet-1, the singlet-2 fluorescence shows a symmetric spectrum compared to the corresponding absorption one (Fig. 10). This alteration confirms the difference between the second and first singlet excited states suggested, on the basis of the degeneration vs. split, the low quantum yield of the internal conversion between them, as well as the dissimilarity between the Soret- and Q-absorption bands.

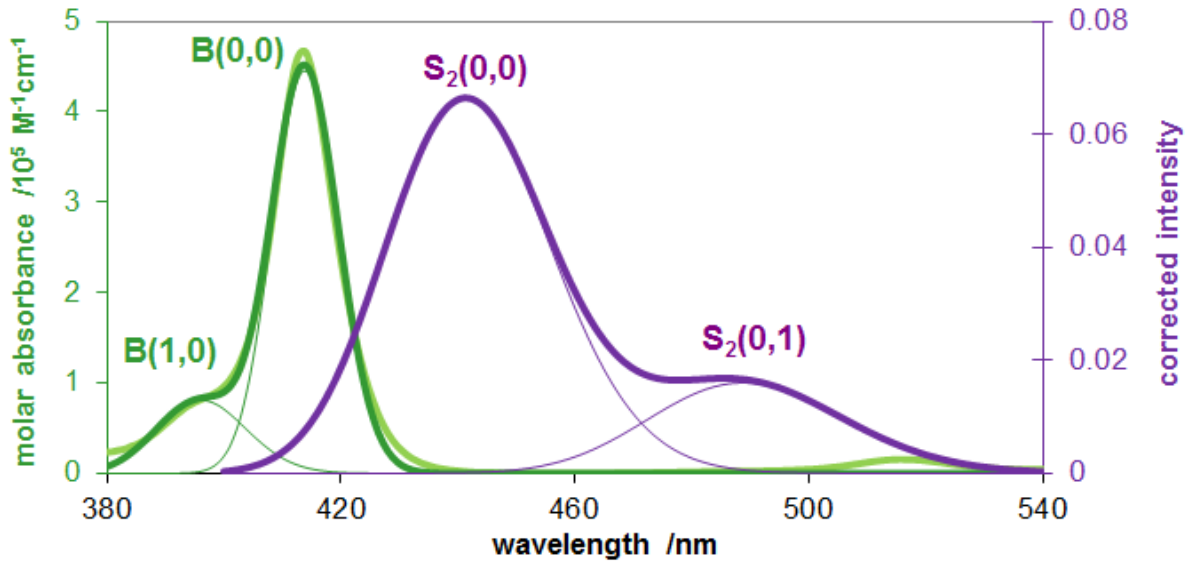

Fig. 10. Singlet-2 fluorescence spectrum of H_2TSPP^{4-} compared to its Soret-absorption spectrum.

The quantum yields of the S_2-fluorescence are extremely low: they are usually 20-60-fold lower than those for the S_1-fluorescence (Table 4) for the metalloporphyrins, but ~1200-fold for the free-base ligand (Table 5); as a consequence of the rigidity increased by the metalation (and the deprotonation too).

Table 5. Characteristic S_2-fluorescence data of the investigated TSPP compounds.

complex	$S_2(0,0)$ /nm	S_2-Stokes-shift /cm^{-1}	$\phi(S_2)$ /10^{-5}	ref.
$Al^{III}TSPP^{3-}$	432	1610	8.2	-
$Pd^{II}TSPP^{4-}$	445	1840	3.1	-
H_2TSPP^{4-}	441	1500	6.3	[78]
$Zn^{II}TSPP^{4-}$	430	430	85	-
$Fe^{II}TSPP^{4-}$	433	610	6.3	[75]
$Bi^{III}TSPP^{3-}$	427	310	79	[78]
$Tl^{I}_2TSPP^{4-}$	427	340	81	-
$(Cl)Tl^{III}TSPP^{4-}$	438	570	3.2	[74]

In the Stokes shifts of the S_2-fluorescence (Table 5), significant (~3-6-fold) difference can be observed between the planar (free-base and in-plane metallo-) and distorted porphyrins (OOP, as well as border-line cases). The Stokes shift is proportional to the structural change during the excitation, hence, the structure of the S_2-excited porphyrins may be close to that of the already in the electronic ground state dome-distorted OOP complexes. Besides, if these Stokes shifts are compared to those of the S_1-fluorescence (in the range of 200-600 cm^{-1} in Table 4), the structural change must be extremely high in planar porphyrins between their singlet-2 excited and ground states. The reason may be their contraction during the S_2-excitation [114], suggested also on the basis of the increase of energy of (skeleton) vibronic origin.
The essence from analytical aspects is the unambiguous determination of the type of the investigated metal ion's complex (typical in-plane or not), owing to the Stokes shift of the S_2-fluorescence. Certainly, an analytical detection method based on S_2-fluorescence can not be too

sensitive, but very size-selective (moreover, the modification of the size of the coordination cavity is possible). On the other hand, the sensitivity may be one order of magnitude higher for the larger metal ions (forming OOP complexes) than the smaller ones (forming in-plane complexes) on the basis of their S_2-fluorescence quantum yields. However, in a detection method based on S_2-fluorescence for larger metal ions, the samples should be excited at wavelengths shorter than that of the B(0,0) absorption band {e.g. at B(1,0) or N-band} to avoid the potential disturbances of the Rayleigh- and Raman-scatterings. Regrettably, along with this decrease of excitation wavelength, the molar absorbance, as well as the sensitivity will be reduced.

Another consequence of the large difference in the Stokes shifts is that the directions of the shifts of the S_2-fluorescence bands invert (according to the Soret-absorption) between the in-plane and out-of-plane complexes (compared to the free-base ligand) (Fig. 11). Furthermore, the ratio between the intensities of the $S_2(0,0)$ and $S_2(0,1)$ bands, i.e. the mirror symmetry (between the absorption and emission spectra) is decreased in the order of OOP > free-base > in-plane porphyrins (Fig. 11), together with the increase of the Stokes shift (Table 5).

The S_2-fluorescence of $H_2TSPPBr_8^{4-}$ is extremely weak, almost undetectable, as a consequence of its highly distorted structure. Therefore, its spectra for the comparison can be not represented in Fig. 11.

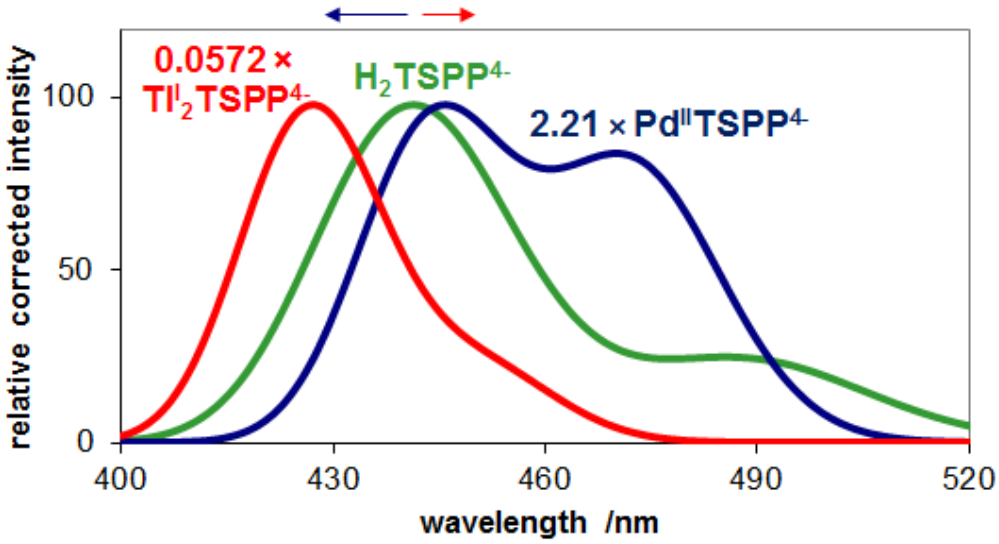

Fig. 11. Singlet-2 fluorescence spectrum of the free-base ligand (H_2TSPP^{4-}), a typical in-plane ($Pd^{II}TSPP^{4-}$) and a typical out-of-plane metalloporphyrin ($Tl^{I}_2TSPP^{4-}$).

4. Conclusion

As conlusions, we emphasize the analytical importance and increments of our spectrophotometric, photophysical, equilibrial, as well as kinetic investigation of water-soluble metalloporphyrins.

- Porphyrins and derivatives are the strongest light-absorbing compounds, therefore the ultraviolet-visible spectrophotometry is one of the most fundamental, yet most informative spectroscopic methods in the porphyrin chemistry.
- In porphyrins the conjugation would favour planar structure, however, geometrical distortion can arise owing to the peripheral substituents or the metal center. “The most

commonly observed spectroscopic consequence of porphyrin nonplanarity is a redshift in the ππ* absorption bands in the UV–visible spectrum."

- We have complemented the categorization introduced by Barnes and Dorough for metalloporphyrins with our experiences regarding the effects of distortion. Accordingly, also in metalloporphyrins, the planarity or nonplanarity of the macrocycle is basically responsible for spectral characteristics, while the electronic structure of the metal center is a secondary factor, with considerable importance mostly in the in-plane complexes.
- The structural as well as the spectroscopic and electronic effects of the metalation for the free-base porphyrins make a highly sensitive detection of metal ions possible, mainly in spectrophotometric methods.
- The UV-Vis absorption bands of in-plane metalloporphyrins are blueshifted, while those of out-of-plane complexes are redshifted compared to those of the corresponding free-base porphyrin. The out-of-plane metallo-monoporphyrins display "common" properties in absorption as well as in fluorescence. Therefore, in a spectrophotometric detection method of metal ions by porphyrins (or by other ringed, chelate ligands), we must presume on a lot of interferences: the metal ions possessing a size above or around the critical value compared to the cavity of the ligand will have similar, almost the same absorption properties.
- The broadenings of absorption bands and the disappearance of fluorescence bands are typical consequences of the formation of bis- or oligoporphyrins. This spectral evidence can be very useful in a metal ion detection method to prove the formation of complexes with various compositions. Hence, the potential deviation of the analytival curve from linearity can be explained.
- Several metal ions can form different types of complexes, depending on the porphyrin, the potential axial ligands as well as the solvent too. This can cause mistakes in a spectrophotometric detection method of metal ions.
- On the basis of the investigation of the complex formation from equilibrial and kinetic aspects, the concentration limit of the metal ion (LoD) and the time required for the complexation, and the detectability (ToD) can be estimated. From the investigation of the complex formation mechanism, we can suggest techniques for the simultaneous decrease of both analytical parameters:
  a) the application of a potential axial ligand in a suitable concentration;
  b) the distortion of the porphyrin ligand by overcrowded substitution on the periphery.
- In a spectrophotometric detection method of Lewis bases as potential axial ligands, an out-of-plane metalloporphyrin may be more suitable if the molecule can form 2:1 (axial ligand:porphyrin) complex with the in-plane metalloporphyrins, and this compound has almost the same absorption spectrum as the initial metalloporphyrins. The presence (or remain) of the axial ligand on the metal center can be confirmed by the strengthening of the Q(0,0) absorption band compared to Q(1,0), as well as the S_1(0,1) fluorescence band compared to S_1(0,0).
- The peripheral substituents of porphyrins can also coordinate to metal ions, therefore, in a detection method, the porphyrin ligand must be carefully chosen for the metal ions.
- The measurement of the less intense charge transfer bands increases the selectivity, but the concentration necessary for their measurability considerably diminishes the sensitivity of an analytical detection method.
- The selectivity of an analytical detection method based on S_1-fluorescence measurements is further reduced compared to the absorptions, as a consequence of the blueshifted fluorescence bands of both types (in-plane and out-of-plane) of metalloporphyrins. Furthermore, the circle of detectable metal ions is more limited in the measurement of fluorescence compared to that of absorption because the highly distorted complexes, the

out-of-plane bisporphyrins and the paramagnetic in-plane complexes do not luminesce at room temperature. Conversely, the paramagnetic border-line cases and out-of-plane complexes have similar fluorescence properties as the diamagnetic ones.

- An analytical detection method based on S_1-fluorescence measurements may be more sensitive than an absorption technique, on the basis of the relatively high emission quantum yields of porphyrins. The spectrofluorometers measure the absolute light intensity emitted by the sample, therefore, the relation between the quantum yield of the internal conversion (between the S_2- and S_1-states) and the ratio between the absorbed light intensity at Soret-excitation and that at Q-excitation determines, which excitation band results in higher sentivity.
- The determination of the quantum yield of internal conversions between the singlet-2 and singlet-1 excited states may be beneficial because the metal ions can be size-selectively detected, the radii of which are around the upper border of the critical region.
- The excitation spectrum must be measured for the identification of the luminescent species.
- The photoreactivity of porphyrins, mainly out-of-plane metalloporphyrins, can cause difficulties, e.g. degradation during a fluorescence detection method.
- The type of the investigated metalloporphyrins (typical in-plane or not) can be unambiguously determined on the basis of the Stokes shift of the S_2-fluorescence. An analytical detection method based on the S_2-fluorescence can not be too sensitive, but very size-selective. On the other hand, the sensitivity may be one order of magnitude higher for the larger metal ions (forming OOP complexes) than the smaller ones (forming in-plane complexes), on the basis of their S_2-fluorescence quantum yields.

Acknowledgments

This work was supported by the Hungarian Scientific Research Fund (OTKA No. K81843 and and K101141) and the Hungarian Government and the European Union, with the co-funding of the European Social Fund (4.2.2/B-10/1-2010-0025).

References

1. A.R. Bettersby, C.J.R. Fookes, G.W.J. Matcham, E. McDonald, Biosynthesis of the pigments of life: formation of the macrocycle, Nature (London) 285 (1980) 17-21.
2. R.H. Garrett and C.M. Grisham: Biochemistry; Saunders College Publishing, Fort Worth, 1999.
3. J.A. Shelnutt, X.-Z. Song, J.-G. Ma, S.-L. Jia, W. Jentzen, C.J. Medforth, Nonplanar porphyrins and their significance in proteins, Chem. Soc. Rev. 27 (1998) 31-41.
4. W.A. Kaplan, K.S. Suslick, R.A. Scott, Core size and flexibility of metallohydroporphyrin macrocycles. Implications for F430 coordination chemistry, J. Am. Chem. Soc. 113 (1991) 9824-9827.
5. Z. Wei, F. Hong, M. Yin, H. Li, F. Hu, G. Zhao, J.W. Wong, Subcellular and molecular localization of rare earth elements and structural characterization of yttrium bound chlorophyll a in naturally grown fern Dicranopteris dichotoma, Microchem. J. 80 (2005) 1-8.
6. R. Bonnett, F. Czechowski, Metals and Metal Complexes in Coal, Philos. Trans. R. Soc. London. Ser. A. 300 (1981) 51-63.
7. C.B. Duyck, T. Dillenburg Saint'Pierre, N. Miekeley, T.C. Oliveira da Fonseca, P. Szatmari, High performance liquid chromatography hyphenated to inductively coupled plasma mass spectrometry for V and Ni quantification as tetrapyrroles, Spectrochim. Acta B. 66 (2011) 362–367.

8. J.R. Miles, P.J. Sarre, On the diffuse interstellar bands, J.C.S. Faraday Trans. 89 (1993) 2269-2276.
9. S. Al-Karadaghi, R. Franco, M. Hansson, J. A. Shelnutt, G. Isaya, G. C. Ferreira, Chelatases: distort to select? Trends Biochem. Sci. 31 (2006) 135-142.
10. Z. Valicsek, O. Horváth, G. Lendvay, I. Kikaš, I. Škorić, Formation, photophysics, and photochemistry of cadmium(II) complexes with 5,10,15,20-tetrakis(4-sulfonatophenyl)porphyrin and its octabromo derivative: the effects of bromination and the axial hydroxo ligand, J. Photochem. Photobiol. A. 218 (2011) 143–155.
11. H. He, Y. Zhong, L. Si, A. Sykes, Structural, photophysical and theoretical studies of two dodecachlorinated porphyrins, Inorg. Chim. Acta 378 (2011) 30–35.
12. N.C. Maiti, S. Mazumdar, N. Periasamy, J- and H-Aggregates of Porphyrins with Surfactants: Fluorescence, Stopped Flow and Electron Microscopy Studies, J. Porph. Phthal. 2 (1998) 369–376.
13. C. Brückner, M.A. Hyland, E.D. Sternberg, J.K. MacAlpine, S.J. Rettig, B.O. Patrick, D. Dolphin, Preparation of [meso-tetraphenylchlorophinato]nickel(II) by stepwise deformylation of [meso-tetraphenyl-2,3-diformyl-secochlorinato]nickel(II): conformational consequences of breaking the structural integrity of nickel porphyrins, Inorg. Chim. Acta 358 (2005) 2943-2953.
14. R. Harada, Y. Matsuda, H. Okawa, R. Miyamoto, S. Yamauchi, T. Kojima, Synthesis and characterization of chromium(III) octaphenylporphyrin complexes with various axial ligands: An insight into porphyrin distortion, Inorg. Chim. Acta, 358 (2005) 2489-2500.
15. K.R. Ashley, I. Trent, Kinetic and equilibrium study of the reaction of [meso-tetrakis(p-sulfonatophenyl)porphinato]diaquachromate(III) with pyridine in aqueous solution, Inorg. Chim. Acta, 163 (1989) 159-166.
16. P.N. Dwyer, L. Puppe, J.W. Buchler, W.R. Scheidt, Molecular stereochemistry of (alpha,gamma-dimethyl-alpha,gamma-dihydrooctaethylporphinato)oxotitanium(IV), Inorg. Chem. 14 (1975) 1782-1785.
17. L. Galich, H. Hückstädt, H. Homborg, Tetra(n-butyl)ammonium Dicyanotetraphenylporphyrinatomanganate(III); Crystal Structure and Electronic Resonance Raman and Absorption Spectra, J. Porph. Phthal. 2 (1998) 79-87.
18. I.H. Wasbotten, T. Wondimagegn, A. Ghosh, Electronic Absorption, Resonance Raman, and Electrochemical Studies of Planar and Saddled Copper(III) meso-Triarylcorroles. Highly Substituent-Sensitive Soret Bands as a Distinctive Feature of High-Valent Transition Metal Corroles, J. Am. Chem. Soc. 124 (2002) 8104-8116.
19. O. Horváth, R. Huszánk, Z. Valicsek, G. Lendvay, Photophysics and photochemsitry of kinetically labile, water-soluble porphyrin complexes, Coord. Chem. Rev. 250 (2006) 1792-1803.
20. O. Horváth, Z. Valicsek, G. Harrach, G. Lendvay, M.A. Fodor, Spectroscopic and photochemical properties of water-soluble metalloporphyrins of distorted structure, Coord. Chem. Rev. 256 (2012) 1531-1545.
21. P.D. Smith, B.R. James, D.H. Dolphin, Structural aspects and coordination chemistry of metal porphyrin complexes with emphasis on axial ligand binding to carbon donors and mono- and diatomic nitrogen and oxygen donors, Coord. Chem. Rev. 39 (1981) 31-75.
22. Z. Valicsek, G. Lendvay, O. Horváth, Equilibrium, photophysical, photochemical and quantum chemical examination of anionic mercury(II) mono- and bisporphyrins, J. Phys. Chem. B. 112 (2008) 14509-14524.
23. N. Kobayashi, Theoretical interpretation of spectroscopic data, J. Porph. Phthal. 4 (2000) 377-379.

24. S. Gentemann , C.J. Medforth, T. Ema, N.Y. Nelson, K.M. Smith, J. Fajer, D. Holten, Unusual picosecond $^1(\pi, \pi^*)$ deactivation of ruffled nonplanar porphyrins, Chem. Phys. Lett. 245 (1995) 441-447.
25. P. Sayer, M. Gouterman, C.R. Connell, Metalloid porphyrins and phthalocyanines, Acc. Chem. Res. 15 (1982) 73-79.
26. J. Barnes, G. Dorough, Exchange and replacement reactions of α,β,γ,δ–tetraphenyl-metalloporphins, J. Am. Chem. Soc. 72 (1950) 4045-4050.
27. A. Valiotti, A. Adeyemo, P. Hambright, Iron(II) and magnesium(II) porphyrin acid solvolysis reactions, Inorg. Nucl. Chem. Lett. 17 (1981) 213-214.
28. M. Biesaga, K. Pyrzynska, M. Trojanowicz, Porphyrins in analytical chemistry. A review, Talanta 51 (2000) 209-224.
29. S. Funahashi, Y. Inada, M. Inamo, Dynamic study of metal-ion incorporation into porphyrins based on the dynamic characterization of metal ions and on sitting-atop complex formation, Anal. Sci. 17 (2001) 917-927.
30. S. Srijaranai, W. Autsawaputtanakul, Y. Santaladchaiyakit, T. Khameng, A. Siriraks, R.L. Deming, Use of 1-(2-pyridylazo)-2-naphthol as the post column reagent for ion exchange chromatography of heavy metals in environmental samples, Microchem. J. 99 (2011) 152–158.
31. X.B. Zhang, C.C. Guo, Z.Z. Li, G.L. Shen, R.Q. Yu, An optical fiber chemical sensor for mercury ions based on a porphyrin dimer, Anal. Chem. 74 (2002) 821-825.
32. K.K. Latt, Y. Takahashi, Fabrication and characterization of a α,β,γ,δ-Tetrakis(1-methylpyridinium-4-yl)porphine/silica nanocomposite thin-layer membrane for detection of ppb-level heavy metal ions, Anal. Chim. Acta 689 (2011) 103–109.
33. A.S. Madison, B.M. Tebo, G.W. Luther III, Simultaneous determination of soluble manganese(III), manganese(II) and total manganese in natural (pore)waters, Talanta 84 (2011) 374–381.
34. S. Igarashi, T. Aihara, T. Yotsuyanagi, Flow injection spectrophotometric determination of ng ml-levels of cobalt (II) using the photochemical decomposition of a cadmium(II) - water-soluble porphyrin complex, Anal. Chim. Acta 323 (1996) 63-67.
35. K. Kawamura, K. Ikoma, S. Igarashi, H. Hisamoto, Toshio Yao, Flow injection analysis combined with a hydrothermal flow reactor: Application to kinetic determination of trace amounts of iridium using a water-soluble porphyrin, Talanta 84 (2011) 1318–1322.
36. K. Kawamura, S. Igarashi, T. Yotsuyanagi, Catalytic activity of noble metal ions for the degradation of 5,10,15,20-tetrakis(4-sulfonatophenyl)porphine in the presence of oxidizing agent, and its application to the determination of ultra trace amounts of ruthenium, Microchim. Acta 172 (2011) 319–326.
37. L.J. Zhou, Z. Cao, J.L. Hu, Z. Peng, P.N. Zeng, G. Su, D.L. He, Fluorescent Determination of Trace Calcium in Water from High-Parameter Power Plant Based on a Porphyrin Derivative, Adv. Sci. Lett. 4 (2011) 1541-1545.
38. L.S. Dolci, E. Marzocchi, M. Montalti, L. Prodi , D. Monti, C. Di Natale, A. D'Amico, Roberto Paolesse, Amphiphilic porphyrin film on glass as a simple and selective solid-state chemosensor for aqueous Hg^{2+}, Biosens. Bioelectron. 22 (2006) 399-404.
39. D. Delmarre, R. Méallet, C. Bied-Charreton, R.B. Pansu, Heavy metal ions detection in solution, in sol-gel and with grafted porphyrin monolayers, J. Photoch. Photobio. A. 124 (1999) 23-28.
40. Y.T. Chen, L. Wan, X. Yu, W.J. Li, Y.Z. Bian, J.Z. Jiang, Rational Design and Synthesis for Versatile FRET Ratiometric Sensor for Hg(2+) and Fe(2+): A Flexible 8-Hydroxyquinoline Benzoate Linked Bodipy-Porphyrin Dyad, Org. Lett. 13 (2011) 5774-5777.

41. H. Mongi, A. Kida, N. Uchida, K. Iwasa, S. Nakano, Determination of lead by stripping voltammetry with a disposable cartridge for quality control of municipal solid waste molten slag, Microchem. J. 97 (2011) 220–224.
42. R. Purrello, S. Gurrieri, R. Lauceri, Porphyrin assemblies as chemical sensors, Coord. Chem. Rev. 190–192 (1999) 683–706.
43. I. Zilbermann, E. Meron, E. Maimon, L. Soifer, L. Elbaz, E. Korin, A. Bettelheim, Tautomerism in N-confused porphyrins as the basis of a novel fiber-optic humidity sensor, J. Porph. Phthal. 10 (2006) 63-66.
44. E.D. Steinle, U. Shaller, M.E. Meyerhoff, Response characteristics of anion-selective polymer membrane electrodes based on gallium(III), indium(III) and thallium(III) porphyrins, Anal. Sci. 14 (1998) 79-84.
45. D.P. Cormode, J.J. Davis, P.D. Beer, J. Inorg. Organomet. Polym. Anion Sensing Porphyrin Functionalized Nanoparticles, 18 (2008) 32–40.
46. M. Tabata, K. Kaneko, Y. Murakami, Y. Hisaeda, H. Mimura, Fluorometric Determination of Trace Amounts of Fluoride Ion Using an Expanded Porphyrin, Microchem. J. 49 (1994) 136-144.
47. V.B. Sheinin, E. L. Ratkova, N.Z. Mamardashvili, pH-dependent porphyrin based receptor for bromide-ions selective binding, J. Porph. Phthal. 12 (2008) 1211-1219.
48. F. Matemadombo, N. Sehlotho, T. Nyokong, Effects of the number of ring substituents of cobalt carboxyphthalocyanines on the electrocatalytic detection of nitrite, cysteine and melatonin, J. Porph. Phthal. 13 (2009) 986–997.
49. X. Zhou, F. Su, Y. Tian, R.H. Johnson, D.R. Meldrum, Platinum (II) porphyrin-containing thermoresponsive poly(N-isopropylacrylamide) copolymer as fluorescence dual oxygen and temperature sensor, Sensor. Actuat. B. 159 (2011) 135-141.
50. J. Chen, L. Zhao, H. Bai, G.Q. Shi, Electrochemical detection of dioxygen and hydrogen peroxide by hemin immobilized on chemically converted graphene, J. Electroanal. Chem. 657 (2011) 34-38.
51. J. Roales, J.M. Pedrosa, P. Castillero, M. Cano, T.H. Richardson, Optimization of mixed Langmuir–Blodgett films of a water insoluble porphyrin in a calixarene matrix for optical gas sensing, Thin Solid Films 519 (2011) 2025–2030.
52. A. Valero-Navarro, J.F. Fernandez-Sanchez, A. Segura-Carretero, U.E. Spichiger-Keller, A. Fernandez-Gutierrez, P. Oña, I. Fernandez, Iron-phthalocyanine complexes immobilized in nanostructured metal oxide as optical sensors of NOx and CO: NMR and photophysical studies, J. Porph. Phthal. 13 (2009) 616–623.
53. I.K. Kim, H.T. Chung, G.S. Oh, H.O. Bae, S.H. Kim, H.J. Chun, Integrated gold-disk microelectrode modified with iron(II)-phthalocyanine for nitric oxide detection in macrophages, Microchem. J. 80 (2005) 219-226.
54. I.M P. de Vargas-Sansalvador, A. Martinez-Olmos, A.J. Palma, M.D. Fernández-Ramos, L.F. Capitán-Vallvey, Compact optical instrument for simultaneous determination of oxygen and carbon dioxide, Microchim. Acta 172 (2011) 455–464.
55. M. Cano, P. Castillero, J.Roales, J.M. Pedrosa, S. Brittle, T. Richardson, A.R. González-Elipe, Angel Barranco, A transparent TMPyP/TiO2 composite thin film as an HCl sensitive optochemical gas sensor, Sensor. Actuat. B. 150 (2010) 764–769.
56. J. Kim, S.-H. Lim, Y. Yoon, T.D. Thangadurai, S. Yoon, A fluorescent ammonia sensor based on a porphyrin cobalt(II)–dansyl complex, Tetrahedron Letters 52 (2011) 2645–2648.
57. J.K. Choi, G. Sargsyan, M. Shabbir-Hussain, A.E. Holmes, M. Balaz, Chiroptical Detection of Condensed Nickel(II)-Z-DNA in the Presence of the B-DNA Via Porphyrin Exciton Coupled Circular Dichroism, J. Phys. Chem. B. 115 (2011) 10182-10188.

58. J.F. Zhai, H.L. Li, X.P. Sun, A novel application of porphyrin nanoparticles as an effective fluorescent assay platform for nucleic acid detection, RSC Advances 1 (2011) 36-39.
59. Y.-X. Ci, Y. Chen, Y.-Z. Li, W.-B. Chang, The use of Mn-TPPS4 mimetic peroxidase in a DNA hybridization assay, Microchem. J. 52 (1995) 257-262.
60. C.Z. Huang, Y.F. Li, P. Feng, Determination of proteins with α,β,γ,δ–tetrakis(4-sulfophenyl)porphine by measuring the enhanced resonance light scattering at the air/liquid interface, Anal. Chim. Acta 443 (2001) 73–80.
61. S.M.A. Pinto, M.A.O. Lourenco, M.J.F. Calvete, A.R. Abreu, M.T.S. Rosado, H.D. Burrows, M.M. Pereira, Synthesis of New Metalloporphyrin Triads: Efficient and Versatile Tripod Optical Sensor for the Detection of Amines, Inorg. Chem. 50 (2011) 7916-7918.
62. M.F. Shao, X.G. Xu, J.B. Han, J.W. Zhao, W.Y. Shi, X.G. Kong, M. Wei, D.G. Evans, X. Duan, Magnetic-Field-Assisted Assembly of Layered Double Hydroxide/Metal Porphyrin Ultrathin Films and Their Application for Glucose Sensors, Langmuir 27 (2011) 8233-8240.
63. S.Y. Zhang, S. Tang, J.P. Lei, H.F. Dong, H.X.; Ju, Functionalization of graphene nanoribbons with porphyrin for electrocatalysis and amperometric biosensing, J. Eletroanal. Chem. 656 (2011) 285-288.
64. D.-G. Kim, M.-W. Jung, I.R. Paeng, J.-S. Rhee, K.-J. Paeng, Solid-Phase Extraction of Phenol and Chlorophenols in Water with a Chemically Modified Polymer-Supported Tetrakis(p-carboxyphenyl) Porphyrin (H2TCPP), Microchem. J. 63 (1999) 134–139.
65. X. Liu, H. Feng, X. Liu, D.K.Y. Wong, Electrocatalytic detection of phenolic estrogenic compounds at NiTPPS|carbon nanotube composite electrodes, Anal. Chim. Acta 689 (2011) 212–218.
66. H. Jeong, H. Kim, S. Jeon, Modified glassy carbon electrode by electropolymerization of tetrakis-(2-aminopheny)porphyrin for the determination of norepinephrine in the presence of ascorbic acid, Microchem. J. 78 (2004) 181–186.
67. M. Svab, M. Svabova, P. Mecirova, Simple determination of nonionic surfactants in highly-polluted aqueous samples, Cent. Eur. J. Chem. 9 (2011) 1150-1157.
68. H. Ibrahim, A. Kasselouri, B. Raynal, R. Pansu, P. Prognon, Investigating the possible use of a tetra (hydroxyphenyl) porphyrin as a fluorescence probe for the supramolecular detection of phospholipids, J. Lumin. 131 (2011) 2528-2537.
69. X.W. Cao, W.Y. Lin, Q.X. Yu, A Ratiometric Fluorescent Probe for Thiols Based on a Tetrakis (4-hydroxyphenyl)porphyrin-Coumarin Scaffold, J. Org. Chem. 76 (2011) 7423-7430.
70. X.Q. Lu, Y.L. Quan, Z.H. Xue, B.W. Wu, H.T. Qi, HT D. Liu, Determination of explosives based on novel type of sensor using porphyrin functionalized carbon nanotubes, Colloid. Surface. B. 88 (2011) 396-401.
71. O. Horváth, Z. Valicsek, A. Vogler, Unique photoreactivity of mercury(II) 5,10,15,20-tetrakis(4-sulfonatophenyl)porphyrin, Inorg. Chem. Commun. 7 (2004) 854-857.
72. Z. Valicsek, O. Horváth, K. L. Stevenson, Photophysics and photochemistry of water-soluble, sitting-atop bis-thallium(I) 5,10,15,20-tetrakis(4-sulfonatophenyl)porphyrin, Photochem. Photobiol. Sci. 3 (2004) 669-673.
73. R. Huszánk, O. Horváth, A heme-like, water-soluble iron(II) porphyrin: thermal and photoinduced properties, evidence for sitting-atop structure, J.C.S. Chem. Commun. (2005) 224-226.
74. Z. Valicsek, O. Horváth, Formation, photophysics and photochemistry of thallium(III) 5,10,15,20-tetrakis(4-sulphonatophenyl)porphyrin; new supports of typical sitting-atop features, J. Photochem. Photobiol. A. 186 (2007) 1-7.

75. R. Huszánk, G. Lendvay, O. Horváth, Air stable, heme-like water-soluble iron(II) porphyrin: in-situ preparation and characterization, J. Biol. Inorg. Chem. 12 (2007) 681-690.
76. Z. Valicsek, G. Lendvay, O. Horváth, Equilibrium, photophysical, photochemical and quantum chemical examination of anionic mercury(I) porphyrins, J. Porph. Phthal. 13 (2009) 910–926.
77. G. Harrach, Z. Valicsek, O. Horváth, Water-soluble silver(II) and gold(III) porphyrins: the effect of structural distortion on the photophysical and photochemical behavior, Inorg. Chem. Commun. 14 (2011) 1756–1761.
78. Z. Valicsek, O. Horváth, K. Patonay, Formation, photophysical and photochemical properties of water-soluble bismuth(III) porphyrins: the role of the charge and structure, J. Photochem. Photobiol. A. 226 (2011) 23– 35.
79. Z. Valicsek, O. Horváth, manuscript in preparation
80. M. Tabata, M. Tanaka, A new method for the determination of the stability constant of metalloporphyrins, use of the catalytic effect of mercury(II) on metalloporphyrin formation, J. Chem. Soc., Chem. Commun. (1985) 42–43.
81. J.R. Platt, Classification and Assignments of Ultraviolet Spectra of Conjugated Organic Molecules, J. Opt. Soc. Amer. 43 (1953) 252-256.
82. J.R. Weinkauf, S.W. Cooper, A. Schweiger, C.C. Wamser, Substituent and Solvent Effects on the Hyperporphyrin Spectra of Diprotonated Tetraphenylporphyrins, J. Phys. Chem. A. 107 (2003) 3486-3496.
83. M. Gouterman, G.H. Wagnière, L.C. Snyder, Spectra of porphyrins: Part II. Four orbital model, J. Mol. Spect. 11 (1963) 108-127.
84. J.A. Shelnutt, Normal-coordinate structural decomposition and the vibronic spectra of porphyrins, J. Porph. Phthal. 5 (2001) 300-311.
85. K. Kalyanasundaram: Photochemistry of Polypyridine and porphyrin complexes; Academic Press, New York, 1992.
86. R.D. Shannon, Revised Effective Ionic Radii and Systematic Studies of Interatomic Distances in Halides and Chalcogenides, Acta Cryst. A32 (1976) 751-767.
87. M. Tabata, K. Ozutsumi, Equilibrium and EXAFS studies of mercury(II) porphyrin in aqueous solution, Bull. Chem. Soc. Jpn. 65 (1992) 1438-1444.
88. M. Tabata, J. Nishimoto, T. Kusano, Spectrophotometric determination of lithium ion using a water-soluble octabromoporphyrin in aqueous solution, Talanta 46 (1998) 703-709.
89. H.R. Jimenez, M. Julve, J. Faus, A solution study of the protonation and deprotonation equilibria of 5,10,15,20-tetra(para-sulphonatophenyl)porphyrin – Stability-constants of its magnesium(II), copper(II) and zinc(II) complexes, J.C.S. Dalton Trans. 8 (1991) 1945-1949.
90. K.M. Barkigia, J. Fajer, A.D. Adler, G.J.B. Williams, Crystal and molecular structure of (5,10,15,20-tetra-n-propylporphinato)lead(II): A roof porphyrin, Inorg. Chem. 19 (1980) 2057-2061.
91. M. Vitasovic, M. Gouterman, H. Linschitz, Calculations on the origin of hyperporphyrin spectra in sequentially protonated meso-(dimethylaminophenyl) porphyrins, J. Porph. Phthal. 5 (2001) 191-197.
92. K.P. Jensen, U. Ryde, Comparison of chemical properties of iron, cobalt, and nickel porphyrins, corrins, and hydrocorphins, J. Porph. Phthal. 9 (2005) 581-606.
93. E.J. Baerends, G. Ricciardi, A. Rosa, S.J.A van Gisbergen, A DFT/TDDFT interpretation of the ground and excited states of porphyrin and porphyrazine complexes, Coord. Chem. Rev. 230 (2002) 5-27.
94. P. Hambright, The coordination chemistry of metalloporphyrins, Coord. Chem. Rev. 6 (1971) 247-268.

95. J.-Y. Jou, C.-H. Chang, G.-H. Lee, Y.Wang, Y. O.Su, W.-L. Yeh, S.-H. Cheng, Electrochemical and resonance Raman studies of nitridomanganese(V) porphyrins in nonaqueous solution, J. Porph. Phthal. 7 (2003) 674-681.
96. M. Radon, E. Broclawik, K. Pierloot, DFT and Ab Initio Study of Iron-Oxo Porphyrins: May They Have a Low-Lying Iron(V)-Oxo Electromer? J. Chem. Theor. Comput. 7 (2011) 898-908.
97. F.F. Pfaff, S. Kundu, M. Risch, S. Pandian, F. Heims, I. Pryjomska-Ray, P. Haack, R. Metzinger, E. Bill, H. Dau, P. Comba, K. Ray, An Oxocobalt(IV) Complex Stabilized by Lewis Acid Interactions with Scandium(III) Ions, Angew. Chem. Int. Ed. 50 (2011) 1711-1715.
98. T. Imamura, T. Jin, M. Fujimoto, Photoreduction of manganese(III), iron(III), cobalt(III), and molybdenum(V) tetraphenylporphyrins in 2-methyltetrahydrofuran, Chem. Lett. 6 (1985) 847-850.
99. M.E. Jamin, R.T. Iwamoto, Gold porphyrin complexes. Evidence for electrochemically inert gold(III), Inorg. Chim. Acta, 27 (1978) 135-143.
100. D.Y. Dawson, J. Arnold, Ionic versus Covalent Bonding in Dilithium Porphyrins: X-ray Structure of Dilithium Tetraphenylporphyrin Bis(etherate), J. Porph. Phthal. 1 (1997) 121-124.
101. P. Hambright, P.B. Chock, Metal-porphyrin interaction III. A dissociative-interchange mechanism for metal ion incorporation into porphyrin molecules, J. Am. Chem. Soc. 96 (1974) 3123-3131.
102. G. Szintay, A. Horváth, Temperature dependence study of five-coordinate complex formation of zinc(II) octaethyl and tetraphenylporphyrin, Inorg. Chim. Acta, 310 (2000) 175-182.
103. T. Yamaki, K. Nobusada, Theoretical study of metal-ligand bonds in Pb(II) porphyrins, J. Phys. Chem. A. 107 (2003) 2351-2355.
104. J.-M. Barbe, C. Ratti, P. Richard, C. Lecomte, R. Gerardin, R. Guilard, Tin(II) porphyrins: Synthesis and spectroscopic properties of a series of divalent tin porphyrins. X-ray crystal structure of (2,3,7,8,12,13,17,18-octaethylporphinato)tin(II), Inorg. Chem. 29 (1990) 4126-4130.
105. N. Schaefle, R. Sharp, NMR-Paramagnetic Relaxation Due to the High-Spin d^3 Electron Configuration: Cr(III)-TSPP, J. Phys. Chem. A. 109 (2005) 3276-3284.
106. M.R. Pereira, J.A. Ferreira, G. Hungerford, Preferential formation of mixed dimers in aluminium containing porphyrin–phthalocyanine systems: A photophysical study, Chem. Phys. Lett. 406 (2005) 360-365.
107. G. Ricciardi, A. Rosa, E.J. Baerends, S.A.J. van Gisbergen, Electronic Structure, Chemical Bond, and Optical Spectra of Metal Bis(porphyrin) Complexes: A DFT/TDDFT Study of the Bis(porphyrin)M(IV) (M) Zr, Ce, Th) Series, J. Am. Chem. Soc. 124 (2002) 12319-12334.
108. Y. Uemori, M. Sakurai, A. Osada, H. Munakata, H. Imai, S. Nakagawa, Synthesis and properties of water-soluble porphyrins bearing multidentate ligands, J. Porph. Phthal. 8 (2004) 1047-1054.
109. P. Seybold, M. Gouterman, Porphyrins XIII: Fluorescence spectra and quantum yields, J. Mol. Spect. 31 (1969) 1-13.
110. G. Szintay, A. Horváth, Five-coordinate complex formation and luminescence quenching study of copper(II) porphyrins, Inorg. Chim. Acta, 324 (2001) 278-285.
111. V.V. Vasil'ev, S.M. Borisov, A. Maldotti, A. Molinari, Spectral properties of cationic water-soluble metalloporphyrins immobilized in a perfluorosulfonated ionexchange membrane, J. Porph. Phthal. 7 (2003) 780-786.

112. D. Wróbel, J. Lukasiewicz, H. Manikowski, Fluorescence quenching and ESR spectroscopy of metallic porphyrins in the presence of an electron acceptor, Dyes Pigments 58 (2003) 7-18.
113. J.S. Baskin, H.Z. Yu, A.H. Zewail, Ultrafast dynamics of porphyrins in the condensed phase: I. Free base tetraphenylporphyrin, J. Phys. Chem. A. 106 (2002) 9837-9844.
114. K. Prendergast, T.G. Spiro, Predicted Geometries of Porphyrin Excited States and Radical Cations and Anions, J. Phys. Chem. 95 (1991) 9728-9736.